Physics of the Earth and Planetary Interiors 168 (2008) 71–87

Contents lists available at ScienceDirect

Physics of the Earth and Planetary Interiors

journal homepage: www.elsevier.com/locate/pepi

Lunar paleointensity measurements: Implications for lunar magnetic evolution

Kristin Lawrence[a,*], Catherine Johnson[a,b], Lisa Tauxe[a], Jeff Gee[a]

[a] Scripps Institution of Oceanography, 9500 Gilman Drive, La Jolla, CA 92093, USA
[b] University of British Columbia, Department of Earth and Ocean Sciences, 6339 Stores Road, Vancouver, British Columbia, Canada V6T 1Z4

ARTICLE INFO

Article history:
Received 7 October 2007
Received in revised form 16 April 2008
Accepted 7 May 2008

Keywords:
Moon
Paleointensity
Remanent magnetism
Thellier–Thellier
sIRM
Lunar dynamo

ABSTRACT

We analyze published and new paleointensity data from Apollo samples to reexamine the hypothesis of an early (3.9–3.6 Ga) lunar dynamo. Our new paleointensity experiments on four samples use modern absolute and relative measurement techniques, with ages ranging from 3.3 to 4.3 Ga, bracketing the putative period of an ancient lunar field. Samples 60015 (anorthosite) and 76535 (troctolite) failed during absolute paleointensity experiments. Samples 72215 and 62235 (impact breccias) recorded a complicated, multi-component magnetic history that includes a low-temperature (<500 °C) component associated with a high intensity (~90 μT) and a high temperature (>500 °C) component associated with a low intensity (~2 μT). Similar multi-component behavior has been observed in several published absolute intensity experiments on lunar samples. Additional material from 72215 and 62235 was subjected to a relative paleointensity experiment (a saturation isothermal remanent magnetization, or sIRM, experiment); neither sample provided unambiguous evidence for a thermal origin of the recorded remanent magnetization. We test several magnetization scenarios in an attempt to explain the complex magnetization recorded in lunar samples. Specifically, an overprint from exposure to a small magnetic field (an isothermal remanent magnetization) results in multi-component behavior (similar to absolute paleointensity results) from which we could not recover the correct magnitude of the original thermal remanent magnetization. In light of these new experiments and a thorough re-evaluation of existing paleointensity measurements, we conclude that although some samples with ages of 3.6 to 3.9 Ga are strongly magnetized, and sometimes exhibit stable directional behavior, it has not been demonstrated that these observations indicate a primary thermal remanence. Particularly problematic in the interpretation of lunar sample magnetizations are the effects of shock. As relative paleointensity measurements for lunar samples are calibrated using absolute paleointensities, the lack of acceptable absolute paleointensity measurements renders the interpretation of relative paleointensity measurements unreliable. Consequently, current paleointensity measurements do not support the existence of a 3.9–3.6 Ga lunar dynamo with 100 μT surface fields, a result that is in better agreement with satellite measurements of crustal magnetism and that presents fewer challenges for thermal evolution and dynamo models.

© 2008 Elsevier B.V. All rights reserved.

1. Introduction

Evidence of an internally generated magnetic field is a crucial constraint for understanding the thermal and dynamical evolution of any planetary body. Although the Moon currently does not possess a core-generated magnetic field (Russell et al., 1974; Sonett et al., 1967), Apollo surface magnetometer and sub-satellite measurements indicated spatially heterogeneous magnetic anomalies, of amplitudes up to 300 nT, interpreted as remanent crustal magnetization (e.g. Fuller and Cisowski, 1987; Hood et al., 1981; Lin et al., 1988). More recently, analyses of Lunar Prospector Electron Reflectometer experiment (Halekas et al., 2003, 2001; Mitchell et al., 2008) and Lunar Prospector Magnetometer experiment (e.g. Hood et al., 2001; Richmond and Hood, 2008) data have confirmed crustal anomalies, with the largest magnitude signals located antipodal to major impact basins (e.g. Lin et al., 1988; Mitchell et al., 2008). Remanent magnetizations in lunar samples, returned during the Apollo missions, provide an opportunity to deduce information about past magnetic field environments. Because no lunar samples, to date, have been unambiguously oriented, paleomagnetic studies focused on paleointensity rather than direction and field geometry.

Paleointensity investigations of nearly seventy lunar samples from 1970 to 1987 using multiple absolute and relative paleointensity measurement techniques, led to the suggestion that the Moon once generated a magnetic field (e.g., Collinson, 1993; Fuller, 1998;

* Corresponding author. Fax: +1 650 725 7344.
E-mail address: klawrence@ucsd.edu (K. Lawrence).

0031-9201/$ – see front matter © 2008 Elsevier B.V. All rights reserved.
doi:10.1016/j.pepi.2008.05.007

Pearce et al., 1972; Runcorn et al., 1971) despite the small size of the lunar core (Hood et al., 1999; Wieczorek et al., 2006). Based on these measurements, Cisowski et al. (1983) and others (Collinson, 1985; Runcorn, 1994; Runcorn, 1996) proposed that from approximately 3.9 to 3.6 Ga, the strength of the lunar surface field was comparable to Earth's present day surface field. Although the high-field paleointensities are often assumed to result from a core dynamo, other mechanisms such as magnetization in a transient field generated by a basin-forming impact may be responsible (e.g. Crawford and Schultz, 1993, 1999; Hood and Artemieva, 2007; Hood and Huang, 1991). Even if the magnetization originated due to a core dynamo field, it is not possible to differentiate between different driving mechanisms, for example, tidal dissipation (Williams et al., 2001) or rapid and transient core cooling (Stegman et al., 2003).

The distribution of lunar paleointensities over time, as summarized by Cisowski et al. (1983), has dictated the predominant view of lunar magnetism. In particular, the thermal implications of an inferred early lunar dynamo have propagated throughout lunar literature (Collinson, 1985; Runcorn, 1994, 1996; Schubert et al., 2001; Stegman et al., 2003). However, interpretation of the existing paleointensity between 3.6 and 3.9 Ga (Fig. 1a) the scatter in measurements during this period is almost two orders of magnitude among different samples, and can be up to an order of magnitude within the same sample. Second, many current lab protocols critical to interpreting an estimated paleointensity as reflecting a primary thermal remanence (i.e., an intrinsic lunar field), were not available at the time the existing data were measured. Third, there is considerable uncertainty in the age that should be assigned to the acquisition of magnetic remanence. Because of the heterogeneous nature of most lunar samples, different radiometric systems record different events within the same sample, and which, if any, of the measured ages is associated with a putative thermal remanent magnetization is unclear. Furthermore, the preferred approach for estimating paleointensity (an absolute measurement—see Section 2 below) involves heating the sample and so a radiometric age must be acquired from a different subsample of the same lunar rock.

In light of significant technical advances made in paleomagnetic techniques and understanding over the past few decades, the interpretation of lunar paleointensity deserves reexamination. This study examines existing lunar paleointensity measurements and contributes new measurements to assess the commonly accepted interpretation of lunar paleointensity data: that of a 3.9–3.6 Ga dynamo. We begin with a brief introduction to paleomagnetic terminology and methodology. We then use objective selection criteria to show that only four absolute intensity measurements from over 30 previously published studies can be considered "reliable". Furthermore, we demonstrate that it is not possible to assess whether any of the published data reflect a primary thermal remanence. We present new paleointensity measurements on four lunar samples (3.3–4.2 Ga) using both absolute and relative techniques. The results are complicated, with multiple magnetic components recorded in lunar samples that can be easily overlooked or misinterpreted with older techniques. We then test several magnetization scenarios in an attempt to explain these complex magnetizations. The non-unique interpretation of the new multi-component results, combined with contamination during sample return (Strangway et al., 1973), and the poorly understood effects of shock, suggest that less sophisticated absolute techniques and relative techniques (e.g., sIRM) incapable of distinguishing between single- and multi-component records, cannot be reliably interpreted. Consequently, current lunar paleointensity data cannot be interpreted as evidence for a primary thermal remanence acquired in a lunar dynamo field.

2. Paleomagnetic methods

2.1. Background

The original orientation of lunar samples is unknown; therefore lunar paleomagnetic studies focus primarily on magnetic sample properties (e.g. mineralogy, and magnetic domain state (e.g. Nagata et al., 1972, 1974; Wasilewski, 1974)), magnitude of magnetization (e.g. natural remanent magnetization, NRM, and paleointensity (e.g. Banerjee and Mellema, 1974; Collinson et al., 1973; e.g. Pearce et al., 1973)), and the possible origin of observed magnetizations (e.g. solar wind (Banerjee and Mellema, 1976) or lunar dynamo (e.g. Cisowski et al., 1982; e.g. Pearce et al., 1972)). Most samples have also been dated with one or more radiometric systems, however the interpretation of these dates is complicated by subsequent shock events. Paleomagnetic studies of lunar samples (summarized by Fuller and Cisowski, 1987; Collinson, 1993) include measurements of Curie temperature (the temperature below which a mineral exhibits long range magnetic order), magnetic susceptibility (the proportionality constant relating an induced magnetization to the inducing field), magnetic anisotropy (variation in magnetization as a function of crystal axis), and coercivity (resistance of a sample to align with an applied magnetic field). From these studies, it is concluded that metallic iron (Fe^0) is the dominant magnetic phase in lunar samples. Since metallic iron is a non-oxidized phase, care must be taken during magnetic experimentation in Earth's atmosphere to ensure that the metallic iron does not oxidize, thereby altering the magnetic carrier. Alloys of metallic iron with nickel (kamacite) and/or cobalt, also contribute experimental complications as they can respectively lower or raise the Curie point of a sample by tens of degrees relative to pure metallic iron (770 °C).

The natural remanent magnetization (NRM) of a sample is the vector sum of all the different possible components of magnetization acquired over its history. Thermal remanent magnetization (TRM) is a type of NRM that arises from magnetic material cooling through the Curie temperature in the presence of a magnetic field. An original TRM is of particular interest because for igneous rocks it records the magnetic conditions at the time of emplacement. Demonstrating a primary TRM origin for the remanence of any sample is difficult. However, high stability to temperature and alternating field demagnetization combined with the decay of the remanence to the origin of a vector-endpoint diagram are necessary requirements for an ancient original TRM.

Estimates of paleointensity fall into two categories: absolute and relative. Absolute techniques rely on replacing the natural remanent magnetization (NRM) by a laboratory-imparted thermal remanence (TRM). Theory then allows the calculation of absolute paleointensity. Relative methods rely on normalization by some non-thermal remanence, and an empirically derived scaling factor must be used to derive an absolute intensity. In the following two sections we provide a cursory description of each approach (see Tauxe and Yamazaki, 2007 for a more detailed summary of paleointensity theory and methods).

2.2. Absolute paleointensity

In some cases, it is possible to estimate the absolute intensity of an original magnetic field in which a sample was magnetized. Thellier (1938) proposed that the intensity of the original field could be determined by assuming a linear relationship between an applied field, B, and a magnetization, M, for each sample: $B = \alpha M$. Assuming the proportionality constant does not change over the range of applied fields a sample is exposed to, ancient fields (B_{anc}) and laboratory-controlled fields (B_{lab}) can be linearly related to the

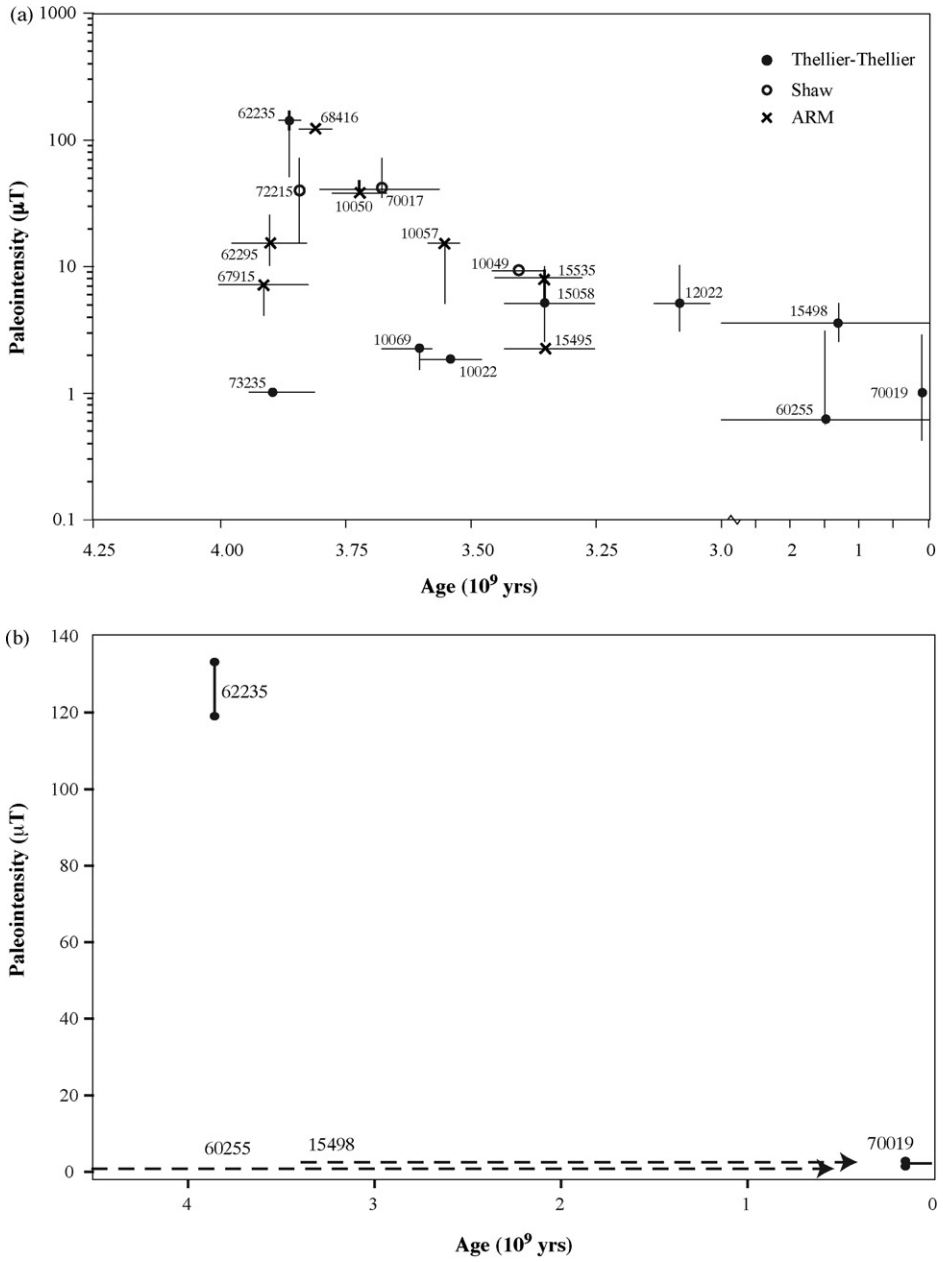

Fig. 1. Paleointensity versus age for lunar samples (a) reproduced from Cisowski et al. (1983) where samples measured using Thellier–Thellier (closed circle), Shaw (open circle) and ARM (×) techniques are labeled with associated sample number. The uncertainties in intensity represent the range in intensity estimates on a given sample as a result of multiple measurement techniques. Ages are determined using a variety of isotope systems and uncertainties represent uncertainty in the best estimate of age. Note the condensed timescale in the age axis at 3 Ga and the *y*-axis is logarithmic. (b) Paleointensity versus age for lunar samples measured using reliable absolute paleointensity measurements (see Supplemental Table A1). The ages are determined using a variety of isotope systems (see text and Supplemental Table A1 for a detailed description). Uncertainty in radiometric age is shown as solid line for each sample while dashed lines represent the range of ages inferred from collection site location (i.e., no radiometric date available). Uncertainties in paleointensity represent ranges in multiple methods as well as individual sample uncertainties.

NRM (M_{anc}) and the laboratory-imparted TRM (M_{lab}) through the following relationship,

$$B_{anc} = \frac{M_{anc}}{M_{lab}} B_{lab}. \quad (1.1)$$

Eq. (1.1) requires that the acquired magnetization of the rock (both in the lab and when originally emplaced) must be reproducible. Two necessary prerequisites for such a reproducible experiment are (1) the presence of uniformly magnetized (single domain) grains in which a remanence acquired at a particular temperature is also completely removed by zero-field cooling from the same temperature and (2) the lack of alteration, which may change the capacity to acquire a remanence, during the paleointensity experiment. Unfortunately, alteration often happens as a result of heating and changes the magnetization properties of a sample such that this relationship is different in the lab than at the time of initial magnetization. Therefore, a good paleointensity procedure should identify the alteration if, and when, it happens. The most commonly employed method today is the double heating Koenigsberger–Thellier–Thellier (Thellier and Thellier, 1959) technique (referred to as KTT in lunar literature and just Thellier–Thellier or T–T in terrestrial studies), during which the sample is heated in a stepwise manner, progressively replacing the original NRM with a laboratory-controlled partial TRM (pTRM).

Thus, the stability of the proportionality (M_{anc}/M_{lab}) can be determined, at least prior to the onset of any alteration.

An important modification to the double heating paleointensity method is the pTRM check, which involves reheating the sample at lower temperatures to check that the remanent magnetization measured at a previous heating step is reproducible. This check therefore monitors changes in the sample's ability to acquire TRM due to alteration. Because it is a modern development, the pTRM check method has not previously been performed successfully for lunar samples.

Our study uses the IZZI variant of the KTT paleointensity experiment (Tauxe and Staudigel, 2004; Yu et al., 2004) to perform an intensity experiment on four lunar samples. In this experiment, the subsamples are heated to a given temperature step and allowed to cool in a zero-field (zero-field step). Next, the specimens are heated to the same temperature and cooled in a field applied along the specimen's cylindrical axis (in-field step). The "zero-field/in-field" method (ZI) of progressively replacing NRM with pTRM allows calculation of the NRM remaining and the pTRM gained after each temperature step through vector subtraction, and is often attributed to Coe et al. (1978). The IZZI method alternates the order of zero-field and in-field measurements (IZ versus ZI) at each temperature step in order to monitor inequalities in blocking and unblocking temperature (the temperature below which material can retain a remanent magnetization despite changes in applied field). This adaptation makes the IZZI method uniquely devised to monitor multi-domain behavior, a non-uniform magnetization state, within the rock and replaces the need for the more time consuming pTRM-tail checks (Riisager and Riisager, 2001).

The methodology outlined above provides a means of evaluating two necessary requirements (remanence carried by single-domain grains and the lack of alteration) for a successful absolute paleointensity experiment. Results from a Thellier–Thellier experiment are traditionally displayed on an Arai plot of NRM remaining versus pTRM gained. An Arai plot representing ideal primary remanence (no secondary overprint), single-domain behavior, and no alteration would have a straight line from which the paleofield could be calculated (Eq. (1.1)).

2.3. Relative paleointensity

To avoid problems incurred through heating of the rock, relative methods have been developed which normalize the NRM by a room temperature magnetic parameter proportional to the magnitude of NRM. The most common relative method used on lunar samples is the sIRM method (Cisowski et al., 1977; Fuller, 1974), which normalizes the NRM with a saturation isothermal remanence (sIRM, sometimes written IRMs). Relative methods also require an empirically derived scaling factor (assuming linearity), f, to estimate the absolute field intensity. The absolute field strength is then calculated as f^* sIRM/NRM. The sIRM is measured after exposing a sample to a (typically 0.6–3 T) magnetic field at room temperature; such a field will saturate the magnetization of the sample. The sIRM method assumes (often inappropriately) that (1) the NRM is a single component remanence, (2) the NRM is an original TRM, (3) the magnetic grains are single domain and isotropic in shape (thereby adhering to Néel theory), (4) the coercivity spectra (strength of magnetization as a function of alternating field strength) of the NRM is similar to that of the IRM. Due to the limitations of these assumptions any relative estimate of paleointensity is at best accurate to within an order of magnitude.

While there have been modifications to the sIRM method (e.g., Gattacceca and Rochette, 2004), none are capable of determining that all assumptions (1–4 above) have been satisfied. The most common adaptation to lunar samples was proposed by Cisowski et al. (1983), and uses a slightly demagnetized value of NRM normalized by a sIRM demagnetized to the same arbitrary AF strength (20 mT) in an attempt to remove unwanted secondary components of magnetization. While it is possible that secondary components are removed, this sIRM adaptation does not verify that the primary component is correctly isolated, nor can it confirm that the primary component is a TRM.

Despite the possibility that relative-to-absolute scaling factors may be dependent upon grain size and mineralogy, several studies have attempted to calculate a single scaling factor for all lunar samples. The approach assumes a linear scaling of relative to absolute intensity that is also independent of field strength. Cisowski et al. (1983) compared absolute paleointensity measurements for 14 lunar samples to corresponding relative measurements to estimate a mineralogy-independent lunar scaling factor ($f = 0.47\ \mu T$), although the data indicate considerable scatter (see Fig. 3 of Cisowski et al., 1983). Kletetschka et al. (2003) proposed another mineralogy-independent scaling factor ($f = 0.3\ \mu T$) based on a combination of synthetic minerals, terrestrial basalts, and the same 14 lunar samples. However, in experiments on five lunar samples Fuller and Cisowski (1987) showed that the scaling of TRM to sIRM varied by a factor of 3 for different rock types and, for four samples, also depended on field strength. More recently, Yu (2006) finds that the scaling factor is dependent on grain size and asserts that mineralogy-dependence has not been sufficiently tested. Consequently, the reliability of either previously proposed single scaling factor for lunar materials is uncertain.

2.4. Paleomagnetic direction

Most studies seek to investigate the original, or primary NRM. However, many mechanisms, including impact related demagnetization/remagnetization (Halekas et al., 2002), thermal events (e.g. Collinson, 1985), or viscous remanent magnetization (Collinson et al., 1973; Sugiura and Strangway, 1980), can overprint or erase the original magnetization. These secondary components of NRM add vectorially to the primary component to produce the total NRM. If the coercivity spectra of these secondary components do not overlap with the primary remanence, they can often be linearly removed through partial demagnetization procedures (thermal or alternating magnetic field). Only through examination of progressive changes in both the direction and magnitude of NRM with increasing demagnetization steps (temperature or field strength) can it be determined that the coercivity spectra do not overlap. In addition, an original primary remanence should also correspond to the highest stability magnetization component. For a paleointensity experiment, this means that the temperature range used to estimate the paleofield should correspond to a magnetization component that trends toward the origin of a vector-endpoint diagram. This is demonstrated by the demagnetization vector having a maximum angle of deviation (MAD) value less than the angle the vector makes with the origin (dANG). Modern paleointensity studies include analyses of both the direction and magnitude of NRM, which is accomplished through a display known as the vector-endpoint diagram (see Butler, 1992, Tauxe, 1998 for discussions of paleomagnetic methods and analyses). Prior to this study, no lunar paleomagnetic experiment used vector-endpoint diagrams to show that the full NRM vector decays linearly to zero, and therefore can be interpreted as the primary (presumably thermal) magnetization recorded by the sample.

Of particular importance, it is possible to add an isothermal remanent magnetization (IRM) through short-term exposure to magnetizing fields (>1 mT or approximately 10 times the Earth's field) at constant temperatures. Strangway et al. (1973) showed that an IRM was acquired in a lunar sample during the return trip

to Earth in the Apollo capsule. Therefore, it is imperative to use a method that can distinguish between primary NRMs and potentially damaging overprints such as the spacecraft IRM.

3. Evaluation of existing paleointensity data

3.1. Previous paleointensity and age compilation

Cisowski et al. (1983) present two distinct compilations of lunar paleointensity. One compilation comprises paleointensities measured using several different paleointensity methods (Fig. 2 of their paper, and recreated here in Fig. 1a); most of these data are absolute paleointensity measurements. The other compilation comprises measurements made using a single technique: the relative paleointensity sIRM technique (their Fig. 7). The sIRM compilation was further assessed by Fuller and Cisowski (1987), and is the one most often reproduced in the lunar literature (e.g. Wieczorek et al., 2006). Here we assess both these previous compilations; however, our primary interest is in the absolute paleointensity data because of the theoretical (Dunlop and Ozdemir, 1997) – rather than empirical – underpinning for such paleofield estimates. In addition, absolute paleointensity estimates have been used to establish the scaling factor (Cisowski et al., 1983) needed to convert sIRM relative paleointensities into an absolute paleofield value (see Section 2.3). Clearly, then, the reliability of the absolute paleointensity data set is of critical importance, since these play a role in the interpretation of all lunar paleointensity results.

3.2. Criteria for acceptable absolute paleointensity data

The paleointensity data shown in Fig. 1a are a recreation of the published absolute paleointensity versus age figure of Cisowski et al. (1983; Fig. 2 in their paper). Due to multiple measurement techniques and within-sample heterogeneity there is a great deal of uncertainty in both the age and proposed paleofield for nearly every sample. The quality criteria applied to the existing database were quite inclusive, allowing the inclusion of both relative and absolute paleointensity measurements.

In this re-evaluation, it is paramount to restrict interpretation of paleointensity data to measurements that represent primary TRM. There are several ways in which intensity experiments may fail to accurately identify a primary TRM; (1) alteration due to grain growth or destruction, (2) magnetic grain interaction at different temperatures, (3) weak and/or unstable remanence, and (4) non-reproducibility of paleointensity measurements. Selkin and Tauxe (2000) identify a set of six criteria that define an acceptable and reliable terrestrial Thellier–Thellier paleointensity measurement. Importantly, there are no published lunar results that pass all of these modern criteria, because the necessary current experimental diagnostics had not been developed (or were not commonly used) when these measurements were made. We define a set of criteria to emulate the stringent terrestrial criteria, but that is more appropriate for the information available for lunar samples.

1. *Absolute methods*: Only methods like the Thellier–Thellier- and Shaw-type methods will be considered for the compilation of absolute paleointensity. Although they were included as absolute measurements by Cisowski et al. (1983) we exclude ARM techniques as published by Stephenson and Collinson (1974) and Banerjee and Mellema (1974). ARM is in fact a relative method and uses a poorly calibrated scaling parameter (Banerjee and Mellema, 1976; Gattacceca and Rochette, 2004). Banerjee and Mellema (1976) argue that it provides estimates of absolute paleointensity with no better than 50% accuracy, which could be due to the chaotic AF (alternating field) demagnetization of kamacite (a prevalent lunar mineral) (Gattacceca and Rochette, 2004).
2. *Published reliability*: In many cases, the authors who publish a paleointensity estimate for a particular sample will provide additional arguments and evidence as to why the estimate is unreliable (e.g. sample 75035 (Sugiura et al., 1978)). A paleointensity estimate is excluded from this study if the publishing authors refute their own estimate for reasons including: evidence of alteration during the experiment, the natural remanent magnetization is (or likely is) not a thermal remanent magnetization, evidence of contamination during sample division (e.g. saw marks), or noted inadequate implementation of technique.
3. *Within-sample reproducibility* (*I*): If the Thellier–Thellier or Shaw method is used, a minimum of four consecutive points must be used to calculate the best-fit line from which paleointensity will be estimated (modification of criteria 3 from Selkin and Tauxe, 2000).
4. *Within-sample reproducibility* (*II*): If a single NRM/pTRM ratio is used, at least three measurements on different pieces of the same sample must agree within 25% of one another. This is an adaptation of criteria 3 applied to a technique that only heats a sample once and then calculates the paleointensity from a total TRM and measured NRM. We consider this method with the stated criteria in an effort to consider the largest data set possible.
5. *Documentation*: A measurement is discarded if it is published without raw data or figures since the quality of the data is then impossible to evaluate. We note that if a sample fails this criterion it also fails one or more other criteria.

These criteria limit the number of acceptable data to four measurements (one less than a similar re-evaluation by Sugiura and Strangway, 1983a). For each of the four acceptable samples, we attempted to determine the best age estimate. The reliability of these age estimates is highly variable, ranging from completely unconstrained (15498 and 60255), a U–Pb concordia diagram (70019), to a well-defined ^{40}Ar–^{39}Ar age plateau (62235). All ages reported in this study have been recalculated (when necessary) using standard radiometric decay constants proposed by Steiger and Jäger (1977). Fig. 1b shows reliable absolute paleointensity measurements versus age without a compressed timescale or logarithmic paleointensity scale as seen in Fig. 1a. Supplemental Table A1 contains a complete reference list and summary of our evaluation of measurement reliability. For some samples in Fig. 1a, we were unable to find published paleointensities (and sometimes ages) that reflect the choice of error bars in the figure. Regrettably, after a thorough search of the literature, we were unable to resolve the cause of such differences.

3.3. Acceptable absolute paleointensity measurements

Here, we provide a brief synopsis of the paleointensity measurements for the four acceptable samples shown in Fig. 1b. Sample 62235 (impact melt breccia) had two successful KTT experiments that yielded reliable intensities of 120 μT (Collinson et al., 1973) and 132 μT (Sugiura and Strangway, 1983a) for temperatures between 0 and ~500 °C. Neither used pTRM checks during the relevant temperature steps, nor reported vector-endpoint diagrams to verify primary remanence. The sample has a well-defined ^{40}Ar–^{39}Ar plateau age of 3.872 ± 0.032 Ga (Norman et al., 2006).

Sugiura and Strangway (1980) performed four paleointensity experiments (ARM, KTT, Shaw, sIRM) on sample 60255 (impact melt breccia) and discuss the reliability of each method. After comparing results of various experiments on a single sample, they conclude that the ARM, Shaw and sIRM measurements are significantly affected by a strong viscous remanent magnetization component.

Although the KTT experiment met the criteria set by this study, the results are considered questionable because of the high scatter in the data, so a paleointensity estimate from this sample of 0.5 μT (temperature steps 500–795 °C) is included with caution. In addition to the tenuous paleointensity result the age estimate for this sample is ill constrained. The possible age range provided in Fig. 1b (dashed line) is merely representative of other Apollo 16 rocks, as no radiometric dates have been published for sample 60255. Nagata et al. (1973) and Sugiura and Strangway (1980) quote a preferred age of 3.9 Ga; we were unable to uncover the reason for Cisowski et al.'s (1983) age of 0–3 Ga (their Fig. 2, our Fig. 1a).

A single KTT experiment was performed on sample 15498 (a glass-coated breccia) (Gose et al., 1973), including a single successful pTRM check at 300 °C, which yielded a well-behaved intensity of 2.2 μT for temperatures between 550 and 650 °C. We note that the published figure by Gose et al. (1973) illustrates an unreported, but much higher intensity associated with temperature steps from 300 to 500 °C. Like sample 60255 there are no published data to verify primary remanence, and the poorly defined age is merely representative of other Apollo 15 results. As with 60255, it is unclear why Cisowski et al. (1983) excluded ages older than 3 Ga as possible ages of this sample.

Sugiura et al. (1979) performed successful KTT experiments on two glassy portions of sample 70019 (a soil breccia). The authors speculated failure in laboratory procedure which possibly resulted in sample alteration above 500 °C but do not have pTRM checks to verify this conclusion. However, if alteration did not occur, then the sample exhibits a multi-component NRM that implies lower intensity associated with high temperature steps above 500 °C. The authors report paleointensities of 1.2 and 2.5 μT for each subsample, which are associated with low-temperature steps (140–470 °C). However, it is impossible to determine whether this paleointensity represents primary remanence as no directional data is provided. The best age estimate (~175 Ma) of this sample is determined from a single U–Pb concordia diagram for measurements on a similar glassy portion of sample 70019 (Nunes, 1975).

3.4. Criteria for acceptable relative paleointensity data

Due to the paucity of acceptable absolute lunar paleointensity measurements, and the abundance of published relative measurements, we provide a cursory re-evaluation of the relative measurements here. The abundance of relative measurements directly results from (1) the ease of relative techniques and (2) the ability to measure paleointensity at room temperature, thereby reducing the risk of alteration during heating. The relative paleointensity compilation of Fuller and Cisowski (1987) has a paleointensity versus age distribution similar to the absolute compilation presented by Cisowski et al. (1983). While uncertainties in both age and intensity are large, only samples with ages between approximately 3.6 and 3.9 Ga were reported to have relatively high intensities (20–100 μT). There is also a lack of data prior to 4 Ga and between 3 and 1.5 Ga. As noted above, relative measurements (including sIRM) are potentially problematic, and require stringent criteria in order to verify that samples are acceptable.

According to Gattacceca and Rochette (2004), relative measurements must pass the following criteria to be considered reliable in a modern experiment. First, any sIRM measurement must be able to differentiate between secondary overprint (IRM), partial demagnetizations (viscous decay, and zero-field shock or heating), and original thermal remanences. Second, as with any reliable paleointensity technique the measurable component of magnetization must decay toward the origin. The sIRM measurements provided by Cisowski et al. (1983), and Fuller and Cisowski (1987) fail both of these criteria because their method cannot differentiate between the components of a multi-component NRM, and there is no published record of directional decay through vector-endpoint diagrams. While there have been more recent measurements by Garrick-Bethel and Weiss (2007), they use the original sIRM method proposed by Cisowski et al. (1983) and do not provide vector-endpoint diagrams of directional data, therefore failing the same criteria. Consequently, there are no verifiably acceptable relative paleointensity measurements with which we can create a modern compilation. Hence, we present two new sIRM measurements on lunar specimens as a comparison to new absolute as well as previous sIRM and absolute paleointensity measurements. Through directional analysis of these new measurements we assess the assumption of primary remanence necessary for a successful sIRM measurement.

3.5. Summary and reinterpretation of paleointensity versus age

Most striking in a comparison of Fig. 1a and b is the absence of reliable data (both in age and absolute paleointensity) resulting from a reexamination of the literature. In the new compilation there is only one reliable lunar sample with a corresponding paleointensity greater than 2.1 μT. The updated compilation also reflects changes in estimated ages relative to those in Cisowski et al. (1983) for two of the samples retained. Samples 60255 and 15498 have no age information, and can only be loosely associated with ages of nearby sites.

Our results have implications for the interpretations of lunar magnetic evolution posited by Cisowski et al. (1983). Despite the great deal of scatter in both age and intensity measurements for samples from 3.9 to 3.6 Ga of Fig. 1a, Cisowski et al. (1983) inferred the presence of an internal lunar dynamo strong enough to produce surface strengths upwards of 100 μT. Based on the assessment presented here, it is clear that the data are insufficient to determine if there was in fact a time interval with an associated high magnetic field intensity, much less the presence or duration of an internal lunar dynamo. Furthermore, if there was a high-field era in lunar history, it is impossible to identify initiation and/or cessation of this era due to the lack of reliable paleointensity data.

4. New lunar paleointensity measurements

Although the lunar paleointensity studies performed in the 1970's provided influential interpretations of lunar magnetism, the results of our compilation make it apparent that new data that clearly demonstrate a primary thermal remanence are needed. New laboratory studies can provide an opportunity to investigate lunar paleointensity with more accuracy and sensitivity simply due to 30 years of improved instrumentation. We present paleointensity experiments for four samples obtained from the Johnson Space Center lunar sample return collection, intended to both bracket (4.3 and 3.3 Ga samples) and fall within the age range of the putative dynamo (3.9 and 3.7 Ga samples). In addition two of our samples are ones for which high paleofield values were previously reported. Unfortunately, experimental requirements of measuring paleointensity will destroy all natural magnetic information of a specimen. It is therefore impossible to perform additional magnetic experiments (e.g. hysteresis), on a sample that was previously used in a paleointensity experiment. Although measuring rock magnetic information on a separate piece of the same lunar sample is possible, within-sample heterogeneity means that the measured properties of one specimen can be different from those giving rise to the observed paleointensity behavior of a different specimen. Due to these restrictions and limited lunar material available to us for this initial study we focus on the reliability of previously

measured and new absolute paleointensity data. The following section contains a brief description of the samples, experimental details, results for absolute and relative paleointensity experiments, and previous magnetic, paleointensity, and age work done on each of the four samples.

4.1. Sample descriptions and previous work

4.1.1. Sample 72215

Sample 72215 is a clast-rich impact melt breccia (see Ryder et al., 1975 for a detailed mineral and petrographic analysis) from Apollo 17. There are no existing double heating paleointensity experiments on this sample. Banerjee and Mellema (1976) performed an unsuccessful Shaw paleointensity experiment on three specimens, while Banerjee and Swits (1975) performed an ARM experiment on another specimens. The best age estimate of this sample is an Ar–Ar measurement of 3.83 ± 0.03 Ga (Schaeffer et al., 1982). We note here that we were unable to determine the decay constant used from the published documentation, but we assume it follows the values outlined by Steiger and Jäger (1977) due to the 1982 publication date. We performed a KTT experiment on specimen 72215.262 and a sIRM experiment on 72215.259. To be consistent with paleomagnetic literature, henceforth we will refer to the smaller pieces of a lunar sample as specimens.

4.1.2. Sample 62235

Sample 62235 is an impact melt breccia (see Crawford and Hollister, 1974 for a detailed mineral and petrographic analysis) from Apollo 16. Sugiura and Strangway (1983a) performed the most recent paleointensity analysis using the Coe-modified Thellier–Thellier method. To reduce alteration during their experiment, specimens were prepared for heating with a two-stage vacuum method proposed by Taylor (1979). Alteration of the sample was monitored by measuring the coercivity of a separate sample that underwent the same heating steps. Modern pTRM checks were not performed in this experiment. As documented above, the best age estimate is 3.876 ± 0.032 Ga (Norman et al., 2006). We performed a KTT experiment on specimen 62235.120 and a sIRM experiment on 62235.118.

4.1.3. Sample 60015

Sample 60015 is a cataclastic ferroan anorthosite from Apollo 16 (see Ryder and Norman, 1980 and its updated online edition http://curator.jsc.nasa.gov/lunar/compendium.cfm for a detailed review of mineral, chemical and petrological studies). There are no existing absolute paleointensity measurements for this sample. However, Stephenson and Collinson (1974) report a single ARM measurement. The best age estimate of this sample is provided by Schaeffer and Husain (1974) as an Ar–Ar plateau age of 3.34 ± 0.04 Ga. This has been recalculated for decay new constants (Steiger and Jäger, 1977). We performed a KTT experiment on specimen 60015.67.

4.1.4. Sample 76535

Sample 76535 is a coarse-grained troctolite from Apollo 17 (see Dymek et al., 1975 for a detailed petrographic description). Textual evidence indicates a slow cooling history and the sample shows little evidence of shock (Gooley et al., 1974). This lunar sample has been dated using a variety of isotopic systems, the most recent and most through analysis is provided by Premo and Tatsumoto (1992) who conclude that the U–Pb date of 4.236 ± 0.015 Ga is most appropriate. No previous paleointensity measurements or magnetic investigations have been made on this sample. We performed a KTT experiment on specimen 76535.136.

4.2. IZZI experimental method

IZZI-modified KTT paleointensity experiments on four lunar specimens were conducted in 50 °C temperature steps until 500 °C followed by smaller temperature increments until >95% of the NRM was lost. Demagnetization and field acquisition in a 15 μT field were performed with custom-built ovens at the Scripps Paleomagnetic Laboratory. Samples were stored continuously in a magnetically shielded room (ambient field <250 nT) for ~3 months prior to the experiment. In an effort to reduce oxidation and subsequent alteration during the experiment, sample preparation included wrapping each specimen in quartz fiber paper (to prevent sample rotation during the lengthy experiment) and sealing the specimen in an evacuated quartz tube (~10^{-4} Torr). Prior to sealing the lunar samples, we verified that the process of sealing the quartz tubes did not contaminate the samples. This preliminary experiment involved giving a test sample of terrestrial submarine basaltic glass a known TRM, sealing it within the test tube, and successfully recovering the intensity (carried by grains with blocking temperatures >100 °C) imparted to the sample prior to the sealing process. We verified that the evacuation technique was effective by demonstrating that copper wool samples encased in the evacuated chambers did not oxidize when heated. All remanence measurements were made using a 2G Enterprises three-axis through-bore cryogenic magnetometer.

Figs. 2–5 display Arai plots, equal area, vector-endpoint, and demagnetization diagrams for lunar specimens 72215.262, 62235.120, 60015.67, and 76535.17, respectively. The temperature steps, intensity, and direction for each step of the IZZI-modified KTT paleointensity experiments can be found in Supplemental Tables A2–A5.

4.3. KTT results

4.3.1. Specimen 72215.262

Lunar specimen 72215.262 shows several interesting, and potentially important, results. Two distinct regions of behavior can be seen in the Arai plot (Fig. 2a) above and below 520–540 °C. These regions will be referred to as slope A (temperatures below 520–540 °C) and slope B (above 520–540 °C). The green triangles represent the pTRM checks performed during the experiment. A failed pTRM check will not fall on or near its associated temperature step (open or closed circle). This specimen passes its pTRM checks, implying no alteration has occurred. The remanent intensity associated with slope B is 1.8 μT, while slope A is associated with an intensity of 103.7 μT. Fig. 2b also supports a change in sample behavior (possibly a change in the magnetic remanence carrier) at 540 °C, at which point the specimen begins to acquire partial remanence in the lab. Interestingly, the specimen loses most of its NRM prior to the temperature where it begins to acquire a measurable pTRM.

A vector-endpoint diagram of direction is shown in Fig. 2c. The directional data define two directions. The first direction, associated with temperature steps 0–520 °C, is well behaved (linear on vector-endpoint diagram) but does not trend toward the origin. The second direction, associated with temperature steps 540–640 °C, is well behaved and approaches the origin, a requirement for a primary remanence. The stability of each direction is less clear in the equal area plot of Fig. 2d.

4.3.2. Specimen 62235.120

As with the previous specimen, 62235.120 displays two distinct regions of behavior (Fig. 3a) above (slope B) and below (slope A) 500 °C. It is likely that this specimen failed a pTRM check at 450 °C, since the pTRM check performed does not fall on or near its

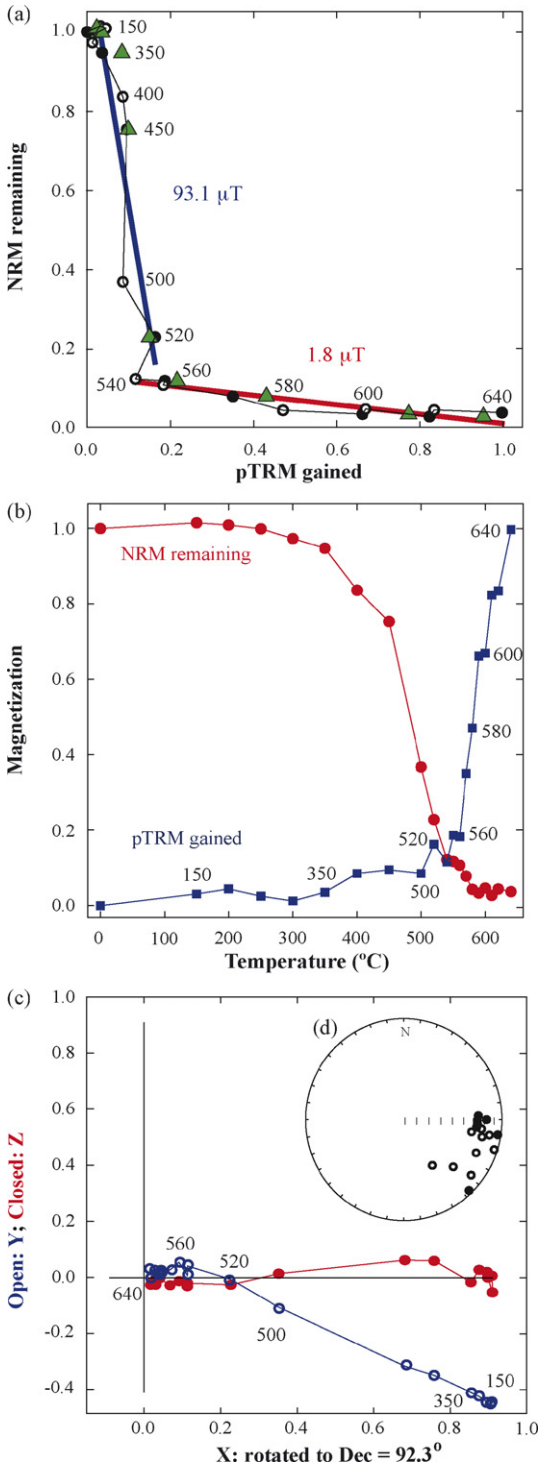

Fig. 2. Paleomagnetic analysis of lunar specimen 72215.262 where the NRM is normalized to a magnetic moment of 3.65E−08 A m^2. Demagnetization steps are labeled in °C. (a) Arai plot of NRM remaining versus pTRM gained during an IZZI-modified T–T paleointensity experiment. Open (closed) circles represent the ZI (IZ) steps of the heating sequence (see text). The red (blue) line represents the inferred paleointensity associated with the high- (low-) temperature steps. pTRM checks (green triangles) are performed at 200, 250, 350, 450, 520, 550, 570, 590, 610, and 640 °C. (b) Demagnetization curve with the NRM remaining displayed as red circles and pTRM gained as blue squares. (c) Vector-endpoint diagram of direction during thermal demagnetization (the zero-field only steps of the T–T experiment) where the *X*-direction has been rotated to the NRM declination, 92.3°, closed circles are the horizontal plane and open circles are the vertical plane. (d) Equal area plot of the direction at each demagnetization step where closed (open) circles represent projections onto the upper (lower) hemisphere.

associated temperature step (filled circle). In addition this specimen exhibits a distinct zigzag shape produced by the alternating red (IZ-step) and white (ZI-step) dots below 500 °C, which likely represents multi-domain behavior, and implies that an intensity value derived from these points is unreliable. If interpreted as reliable despite non-reciprocal behavior of magnetization (elucidated by the zigzag pattern in the Arai plot), slope A yields a paleointen-

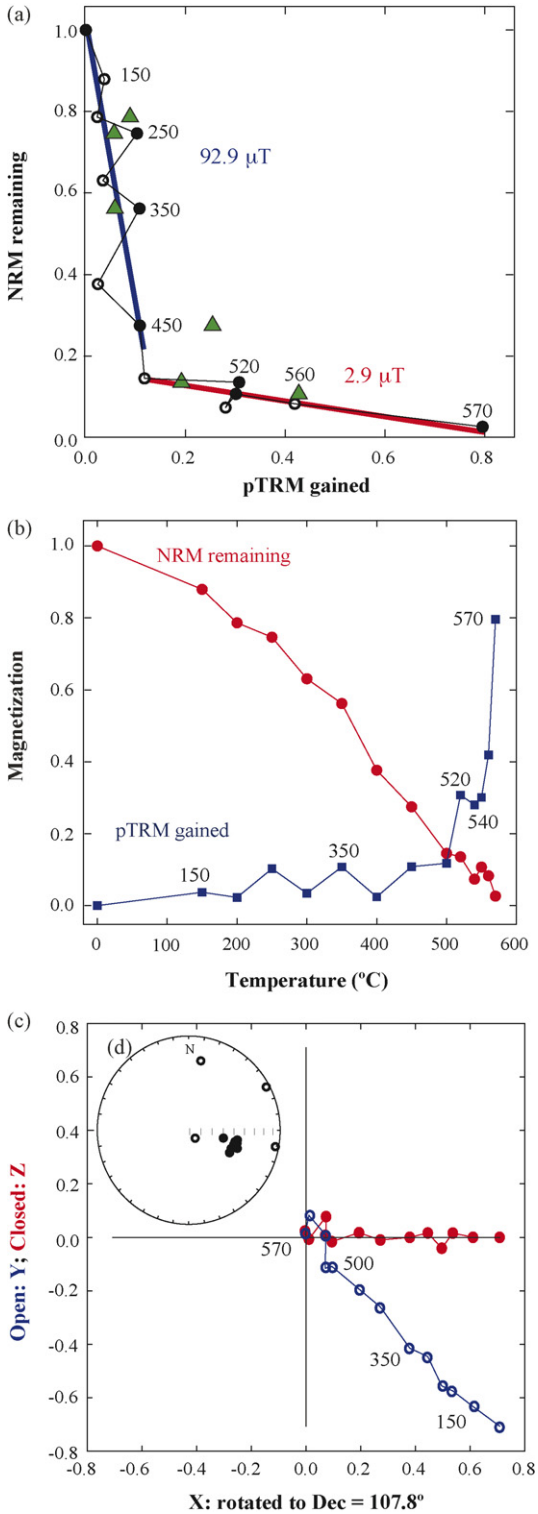

Fig. 3. Same as Fig. 2 for lunar specimen 62235.120 where the NRM is normalized to 4.00E−08 A m^2 and the *X*-direction has been rotated to the NRM declination, 107.8°.

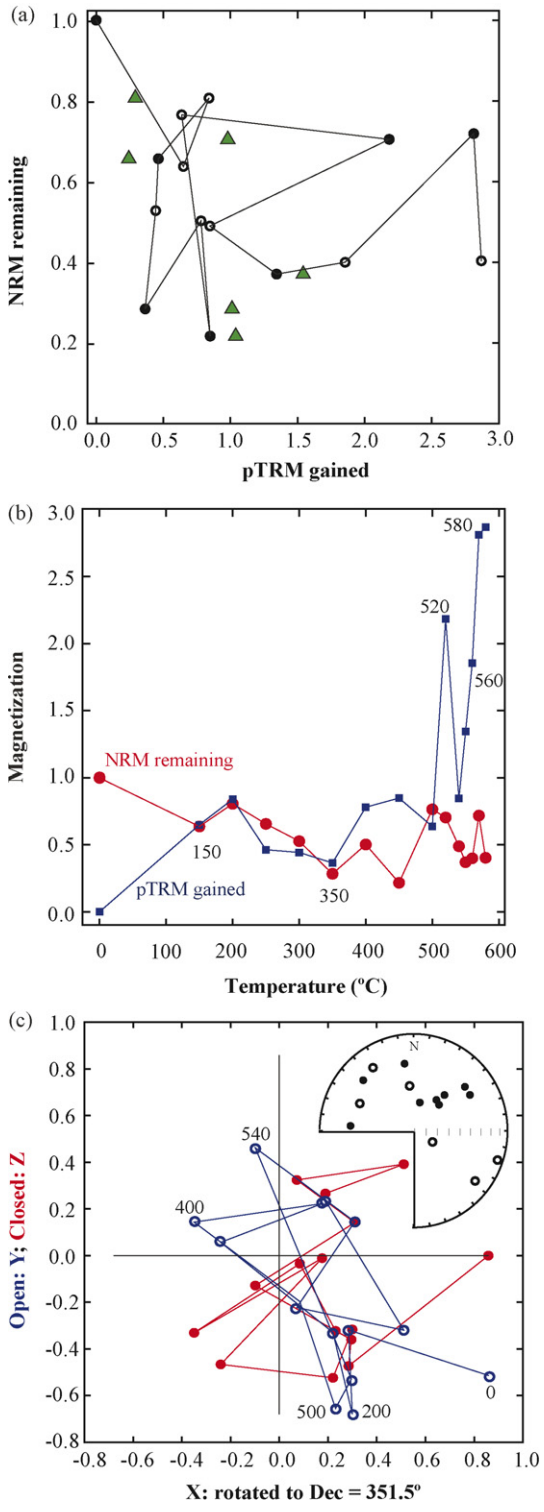

Fig. 4. Same as Fig. 2 for lunar specimen 60015.67 where the NRM is normalized to 1.54E−10 A m^2 and the *X*-direction has been rotated to the NRM declination, 351.5°.

sity estimate of 92.9 μT. Slope B exhibits a linear trend (red line), with little zigzag behavior, and passes pTRM checks. The remanent intensity associated with slope B is 2.9 μT. However, the failed pTRM check at 450 °C, suggests that alteration has occurred, and caution is needed in interpretation of the Arai plot at higher temperatures. The remanence acquisition of 62235 is similar to 72215 since the specimen loses most of its NRM below the same approximate temperature (520 ± 20 °C) at which it gains the majority of its experimentally induced remanence (Fig. 3b). Again, the change in remanence occurs at the same temperature where the slope changes on the Arai plot.

A vector-endpoint diagram of direction is shown in Fig. 3c. The directional data define two directions. The first direction, defined by temperature steps 0–500 °C, is well behaved (linear on vector-

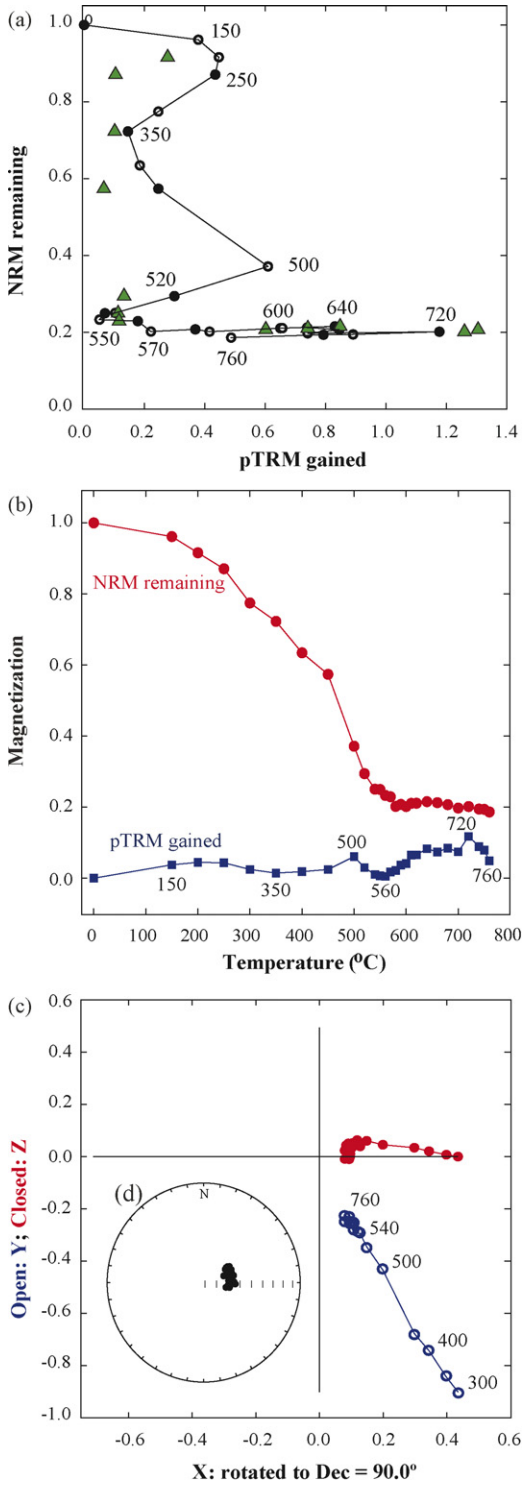

Fig. 5. Same as Fig. 2 for lunar specimen 76535.17 where the NRM is normalized to 2.57E−08 A m^2 and the *X*-direction has been rotated to the NRM declination, 90.0°.

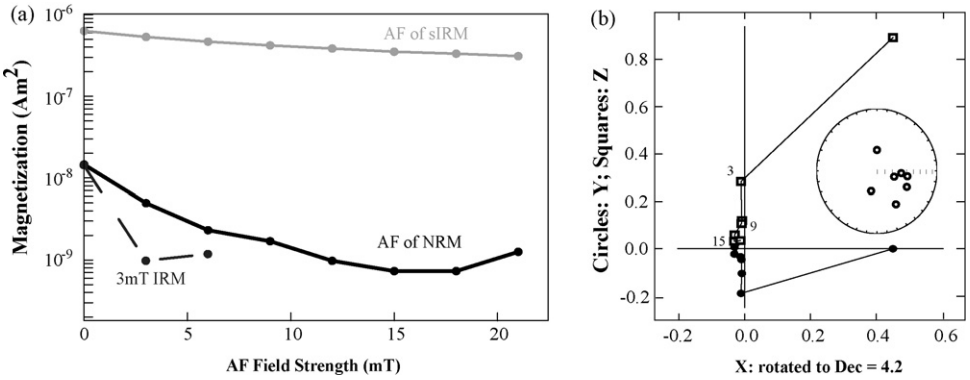

Fig. 6. (a) Alternating field (AF) demagnetization of sample 72215.259 using steps of 3 mT following the GRM protocol outlined by Stephenson (1993). The average of the measurements for each demagnetization step of the NRM (sIRM) are shown in black (grey). The sample was also subjected a 3 mT IRM and demagnetized (shown as a dashed line). (b) Vector-endpoint diagram of demagnetized direction of NRM with the *X*-direction rotated to 4.2°. Inset is an equal area plot of the direction each demagnetization step of the NRM.

endpoint diagram) and approaches the origin. The second direction, defined by temperature steps 500–570 °C, is erratic and it is difficult to determine a clear associated direction. The stability of the first direction is seen in the equal area plot of Fig. 3d.

4.3.3. Specimen 60015.67

The original IZZI-modified Thellier–Thellier experiment specimen 60015.67 failed. The specimen readily demagnetized at low temperature and quickly became too weak to measure. The directions associated with the measured demagnetization steps are unstable and do not yield a coherent component of magnetization. The results from this experiment are displayed in Fig. 4.

4.3.4. Specimen 76535.17

The paleointensity experiment for specimen 76535.17 was unsuccessful. The specimen fails nearly all of the pTRM checks performed (Fig. 5a), including those at lower temperature steps. From temperature steps 0–540 °C the specimen steadily demagnetizes to 20% of its original NRM. The directions associated with temperature steps 0–540 °C are very stable and uni-directional (Fig. 5c and d). The paleointensity experiment on specimen 76535.17 was terminated after temperature step 770 °C since nearly all pTRM checks failed and the specimen was no longer losing NRM or gaining pTRM in a regular fashion (Fig. 5b). Interestingly, the pattern of NRM remaining versus pTRM gained is similar to the results from a paleointensity experiment done on sample 62235 by Pearce et al. (1976). The failure at low temperature (∼300 °C) is most likely due to magnetic interactions of troilite and metallic iron (Pearce et al., 1976), whereas the failure at higher temperature (>600 °C) is likely due to reduction of ilmenite to iron and rutile (Pearce et al., 1976).

4.4. sIRM experimental method

Results from an SIRM experiment on two lunar specimens (72215.259 and 62235.118) are also presented. The NRM of each specimen was demagnetized using a Sapphire Instruments SI-4 alternating field demagnetizer using a triple demagnetization scheme (Stephenson, 1993) whereby specimens are demagnetized along all three axes, measured and then demagnetized along the *y*-axis, measured and then demagnetized along the *z*-axis. At every demagnetization field strength, an average of the three measurements is calculated to counteract the effect of gyroremanent magnetization (GRM). GRM is an unwanted remanence produced during demagnetization due to anisotropy in the orientation of the easy axes of magnetization. Specimens were demagnetized in steps of 3 mT until 80% of the NRM was demagnetized, followed by coarser steps until the magnetization was no longer stable. Exposing the demagnetized specimens to a 1 T field using an ASC Pulse Magnetizer induced saturation remanence. The sIRM was demagnetized with the same protocol applied to the corresponding NRM. The individual measurements of direction and intensity for each level of demagnetization are reported in Supplemental Tables A6–A9.

4.5. sIRM results

4.5.1. Specimen 72215.259

The NRM coercivity spectrum for specimen 72215.259 is very soft and is completely demagnetized by 21 mT (Fig. 6a). A soft component of magnetization is suggestive of an IRM. This interpretation is supported by the fact that all that is necessary to recreate the originally measured NRM is a 3 mT IRM (dashed line in Fig. 6a). The direction of NRM as shown in Fig. 6b also displays an unstable NRM. The specimen begins to exhibit GRM behavior after 15 mT at which point the average NRM and direction of the three demagnetized axes markedly vary (this may be a subtle change in Fig. 6 because multiple measurements have been averaged, see the raw data in Supplemental Table A6 for complete results). The NRM/sIRM ratio (i.e., at 0 mT demagnetization level) for specimen 72215.259 is 0.023. The method proposed by Cisowski et al. (1983) involves the estimation of the NRM/sIRM ratio at 20 mT, but is inappropriate here since the specimen has been completely demagnetized by 20 mT.

4.5.2. Specimen 62235.118

The NRM coercivity spectrum of specimen 62235.118, as shown in Fig. 7a is well behaved and directionally stable until ∼65 mT. GRM behavior is observed after 40 mT. Qualitatively the NRM curve looks similar to an IRM curve. The NRM/sIRM ratio (at 0 mT) for specimen 62235.118 is 0.018 while applying the partial demagnetized method proposed by Cisowski et al. (1983) yields a NRM(20 mT)/sIRM(20 mT) ratio of 0.019.

5. Possible magnetization scenarios

The apparent multi-component nature (slopes A and B for samples 72215 and 62235) of the new absolute paleointensity results (Section 3) is more difficult to interpret than single-component, well-behaved Thellier–Thellier measurements. Here we consider several scenarios in which one, both or neither component of the Thellier–Thellier analysis is an accurate representation of a field(s) present during a portion of the sample's history. Although it is pos-

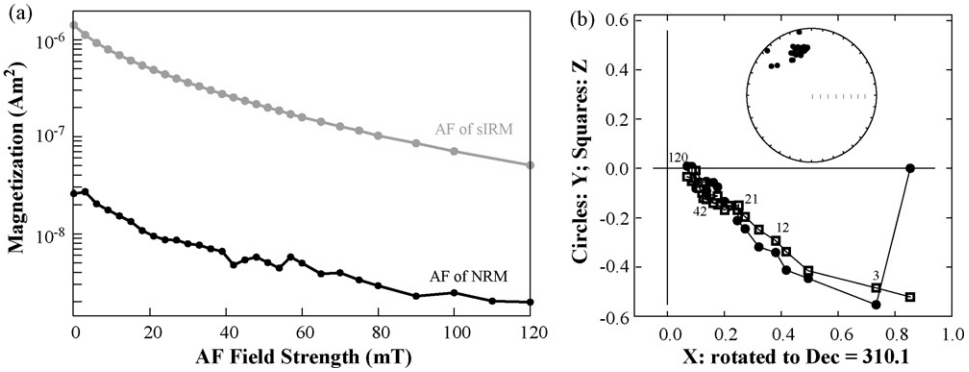

Fig. 7. Same as Fig. 6 for sample 62235.118 where the direction of NRM is rotated to 310.1°.

sible that either or both slopes are erroneous measurements due to experimentation error, alteration, or nonlinear magnetization, our experiments show no conclusive evidence for any of these cases. Therefore, we examine the possibility that both slopes represent one or more records of magnetic events.

First, we hypothesize that samples 72215 and 62235 could each contain two distinct populations of magnetic carriers with different magnetization proportionality constants and blocking temperature spectra, which could result in two slopes produced simultaneously during a single magnetization event. We test this case (Case 1) through thermal acquisition and controlled KTT experiments. Second, it may be possible for multiple magnetizing events due to different mechanisms (TRM, IRM, etc.) to cause slopes A and B even with a single population of magnetic carriers. In this scenario (Case 2), we attempt to differentiate between the various possible mechanisms through KTT experiments with known TRM origins and subsequent exposure to controlled secondary IRM overprint in the lab.

5.1. Case 1: Single magnetization event

A paleofield interpretation of any component of the Arai plot requires that we validate an assumption of the Thellier–Thellier experiment—that of linear acquisition of magnetization with applied field (Section 2.2). After completion of the initial IZZI-modified KTT experiment, specimens from samples 62235 and 72215 were repeatedly heated to temperatures above which the specimens were completely demagnetized and cooled in the presence of magnetic fields of increasing strength. The results of this test verify that both specimens linearly acquire magnetization in fields ranging from 5 to 70 μT. It is likely that even in fields up to 100 μT, our specimens will not violate the linearity assumption of the Thellier–Thellier experiment.

The most direct way to test whether the two-component character of the KTT experimental result originates from a single magnetization event is to repeat the experiment with a known TRM. We heated three of the four specimens demagnetized in the original KTT experiment (72215.262, 62235.120, 60015.67) to 640 °C and cooled them in a 5 μT field. We repeated the KTT experiment, the results of which are shown in Fig. 8. The linear Arai plots of all three specimens strongly indicate that if a sample cooled in the presence of a 5 μT field the sample would respond in a linear way, inconsistent with the hypothesis of two carriers. Since the samples behave in a linear fashion for fields ranging from 5 to 70 μT, the same conclusion can be made for high fields. These two independent experiments strongly indicate that scenario 1 (the sample has two different carriers from which a single magnetization event is expressed by two slopes in the IZZI experiment) is improbable. Although the result in Fig. 8 indicates that specimen 62235.120 can still faithfully record an applied field, the type and extent of alteration is unknown (we noted previously that it probably altered in the original KTT experiment) and so we do not conduct further experiments on this specimen.

Interestingly, sample 60015, which did not have a measurable remanence during the original KTT experiment, may be capable of recording a field as low as 5 μT. Assuming that the specimen did not alter in the original KTT experiment, the results of the controlled TRM experiment (Fig. 8c) indicate that after cooling in the presence of a 5 μT field, it was possible to faithfully recover the strength of the magnetizing field present. Combining the results in Figs. 8c and 4 we infer that the sample was never exposed to a core-field of lunar origin, at or after its Ar–Ar age of ~3.3 Ga.

5.2. Case 2: Secondary IRM overprint

We next test the effect of a secondary IRM on the record of a hypothetical original thermal remanence in a Thellier–Thellier experiment. This experiment is motivated by results presented by Strangway et al. (1973) concerning the magnetic environment the samples were exposed to during the return trip to Earth. After sending a demagnetized Apollo 12 sample on a round trip with Apollo 16, Strangway et al. (1973) concluded that the Apollo samples must have been exposed to an IRM on the order of 3–5 mT, while aboard the Apollo Command Module.

During our controlled TRM + IRM experiment specimen 72215.259 was heated to and cooled in a 5 μT field, thereby imparting a TRM of known magnitude. The specimen was then exposed to an IRM in an arbitrary direction and with strength necessary to recreate the original NRM. The magnitude of a secondary IRM necessary to recreate the original NRM is 4.5 mT, which is within the range specified by Strangway et al. (1973). The specimen was then subjected to another KTT experiment (Fig. 9). Similar to the results presented in Section 3 (Figs. 2a and 3a) the Arai plot in Fig. 9 also displays a two-component nature. The behavior is not identical to that observed in the original KTT experiments, because the change in slope occurs near 300 °C and not 500 °C. The low-temperature slope corresponds to intensity between 30 and 50 μT, while the high-temperature slope is consistent with a 1.8 μT field. The high-temperature slope does not accurately reflect TRM of 5 μT given to the specimen at the outset of the experiment. Most importantly, the specimen does not fail pTRM checks implying that no alteration has occurred. Therefore, our failure to recover the TRM is a result of the IRM overprint.

This controlled IRM overprint experiment is not the only experiment that indicates an IRM as a major component of the original NRM. The sIRM experiment performed on specimen 72215.259 in

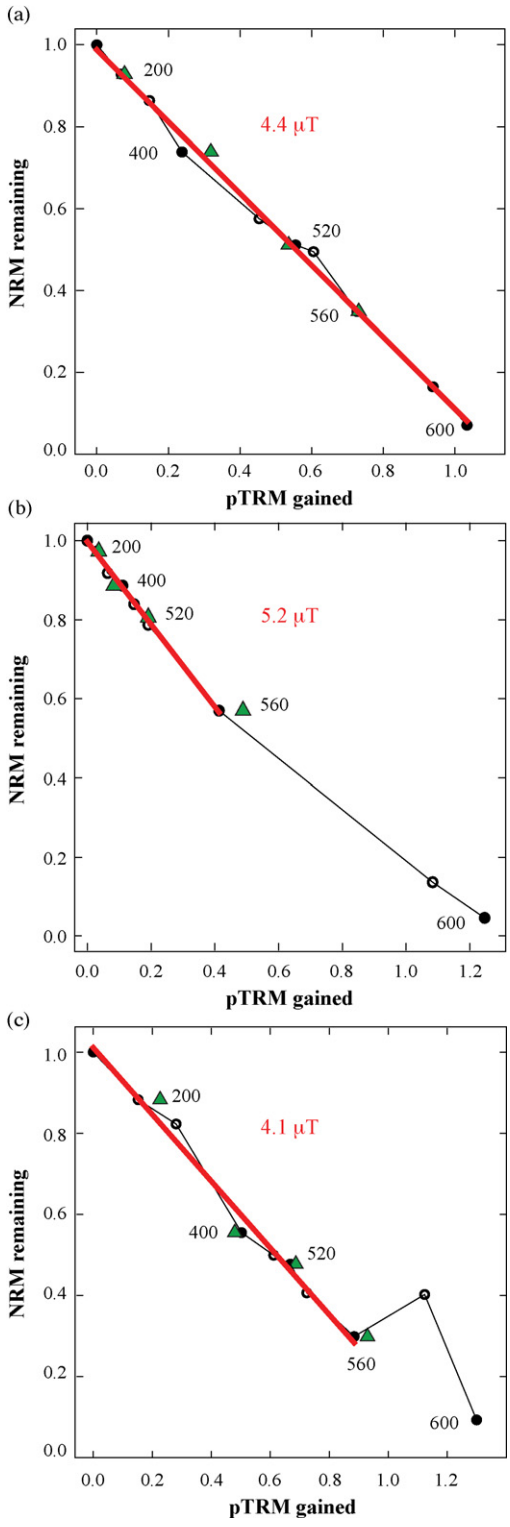

Fig. 8. Results from a Thellier–Thellier experiment performed after samples (a) 72215.262 (b) 62235.120 (c) 60015.67 were completely demagnetized and subsequently cooled in a 5 μT field. Results presented as Arai plots using notation conventions defined for Figs. 2–5. Red lines represent the best estimate of intensity recorded by each sample.

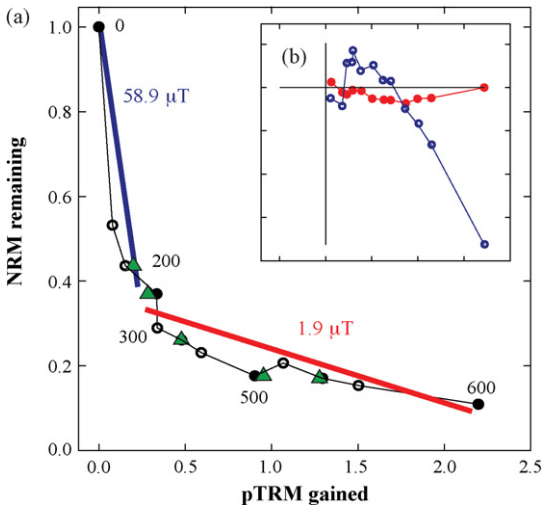

Fig. 9. Results from a Thellier–Thellier experiment performed on sample 72215.262 after being completely demagnetized, cooled in a 5 μT field and then exposed to a 4.5 mT magnetic field. (a) Results presented in an Arai plot using notation conventions defined for Figs. 2–5. The red and blue lines represent the best estimate of intensity for two portions of the Arai plot. Intensity is normalized to 3.09E−8 A m^2. (b) Vector-endpoint diagram of direction associated with each demagnetized step. Red dots (blue circles) represent the x–z (x–y) plane.

this study also indicates an IRM origin for the NRM. The coercivity spectrum of specimen 72215.259 is very soft, having been completely demagnetized by 20 mT (Fig. 6), suggesting a non-thermal origin for the remanence. In addition to the demagnetization characteristics, the observed NRM was reproducible with a 3 mT IRM.

From this controlled experiment it is apparent that the overprint of even a small IRM (much less than saturation IRM) will adversely affect the blocking temperature spectrum of a specimen, leaving it impossible to accurately recover the intensity of the original TRM. This result has a profound impact on the interpretation of lunar paleointensity. It calls into question the validity of previous KTT results as well as the interpretation of relative intensity methods

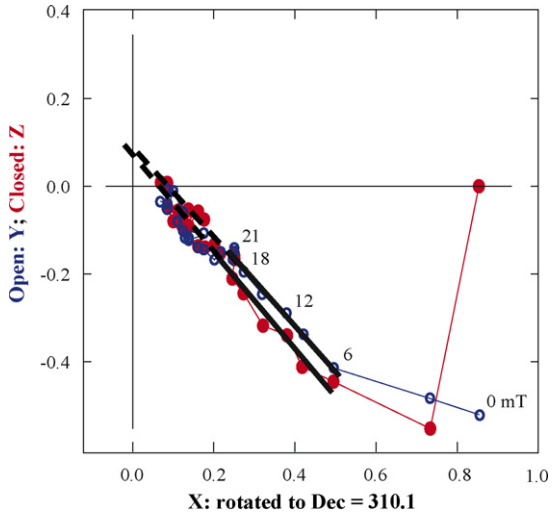

Fig. 10. Vector-endpoint diagram of direction during alternating field demagnetization of sample 62235.118 where the NRM is normalized to 2.60E−8 A m^2 and X-direction has been rotated 310.1°. Closed circles are the horizontal plane and open squares are the vertical plane. Black lines represent the best-fit direction calculated using principal component analysis between 6 and 21 mT demagnetizations steps. Dashed lines linearly extrapolate the calculated trend.

such as sIRM, because of the use of KTT data in establishing the relative-to-absolute scaling factor.

6. Discussion

6.1. Interpretation of paleointensity experiments

6.1.1. Previous studies

The re-evaluation of the published lunar paleointensity data in light of improved measurement techniques shows that paleointensities recorded by lunar samples are not as unambiguously determined as previously thought. We have shown that only four absolute paleointensity measurements meet a set of objective selection criteria (Fig. 1b); these criteria require (a) documentation of original data, (b) no evidence of alteration, and (c) some measure of within-sample reproducibility. Of the four samples, only one has a reported high intensity (62235). Additionally, there are no relative paleointensity data for which the published experimental results currently allow the NRM to be unambiguously interpreted as a primary TRM. Specifically for sIRM measurements, the technique of choice for lunar samples, vector-endpoint diagrams are not routinely displayed with earlier analyses of Apollo samples. In addition, the use of the ratio of NRM to sIRM at an AF demagnetization level of 20 mT to determine a relative paleointensity need not reflect any one of the multiple components of magnetization present in the sample.

Our new paleointensity experiments on sample 62235 produce Arai plots with two distinct slopes. Careful examination of the published literature shows that other studies have also observed this behavior, with a change in the slope of NRM lost versus pTRM gained, at or above 500 °C (Gose et al., 1973; Sugiura and Strangway, 1980, 1983a; Sugiura et al., 1979). This indicates multiple components of magnetization and previous studies analyzed the results in different ways: some interpreting the high-temperature component, and others interpreting the low-temperature component. The low-temperature steps yield paleointensity estimates consistent with previously proposed high-field values for the moon, whereas paleointensities derived from the high temperature steps are an order of magnitude lower and consistent with previously published low field values. For example, Gose et al. (1973) determine low intensity for temperature steps above 500 °C of sample 15498 whereas interpretation of their temperature steps below ~500 °C would yield a much higher intensity. Given this multi-component behavior, it is essential to demonstrate which component (if either) is associated with an original thermal remanence.

6.1.2. New experiments

The controlled TRM experiments (Section 5.1) indicate that three of our samples are capable of accurately recording a primary thermal remanence in applied magnetic fields that span the range of proposed low and high lunar fields. Our new experiments show that three modern laboratory protocols, unavailable or not routinely used in the 1970s, are critical to the interpretation of absolute paleointensity data: these are the simultaneous measurement of paleodirection during the Thellier–Thellier experiments (also essential for relative paleointensity methods), the use of pTRM checks (to detect alteration), and the IZZI approach (to detect non-reciprocal blocking and unblocking behavior).

Of the new measurements, samples 62235 and 72215 show multi-component Arai plots with associated intensities of ~90 μT (low temperature) and ~2 μT (high temperature), which are equivalent to the high intensity assertion from Sugiura and Strangway (1983a) for sample 62235 and the low intensity assertion of Gose et al. (1973) for sample 15498. Because of our detailed laboratory procedures, we are able to investigate whether either component is clearly a primary thermal remanence. We summarize the implications of both our absolute and relative paleointensity experiments on these samples below.

Specimen 62235.120 has well-behaved directions (low scatter) that linearly decay toward the origin at temperature steps lower than 500 °C (Fig. 3c). Yet, the measurements of NRM remaining versus pTRM gained (Arai plot in Fig. 3a) exhibit a strong zigzag characteristic, often indicative of multi-domain magnetic carriers, which are unreliable recorders of magnetic field. It is the use of the IZZI method that allows the detection of this non-reciprocal magnetization/demagnetization behavior; without it the low-temperature portion of the Arai plot would appear linear and well-behaved, resulting in a confident interpretation of a high paleofield value. The use of pTRM checks indicates that the specimen altered at 450 °C, likely leaving the high temperature component of the specimen uninterpretable.

The sIRM results for specimen 62235.118 are also complicated. There is an overprint of unknown origin that is removed by 6 mT (Fig. 7). The specimen directions are then relatively stable until ~21 mT, but the direction does not linearly decay to the origin. This is clearly seen by the dashed lines extending the trend of demagnetization steps 6–21 mT in Fig. 10. In addition, the maximum angle of deviation (MAD = 5.2°) of the best-fit direction for this component is less than the angular difference the component makes with the origin (dANG = 5.6°). The failure of the best-fit directions to decay to the origin indicates that it is not a primary remanence, and that the sIRM measurement does not accurately record the field intensity at the time of sample formation. In summary, any postulate of a high-field era based solely on sample 62235 cannot be substantiated by comparison with previous sIRM results on the same sample, because these earlier studies neglected to prove primary remanence of the observed remanent magnetization.

The results from specimen 72215.262 also do not support a high-field interpretation. The KTT results do not exhibit the same zigzag nature at low temperature as specimen 62235.120. However, the direction associated with these low-temperature steps does not decay linearly to the origin (MAD = 7.2, which is less dANG = 7.7). The high-temperature steps are associated with a lower intensity by a factor of 50 (1.8 as compared to 93.1 μT) and a direction that trends to origin (Fig. 2c) but is relatively unstable (Fig. 2d). In addition, the sIRM results from specimen 72215.259 strongly suggest an IRM origin of remanence since the NRM is completely demagnetized by 20 mT.

6.2. Possible sources for multiple components of magnetization

6.2.1. IRM

Meaningful paleofield interpretation of paleointensity experiments requires that the paleointensity estimate be associated with a primary TRM. The primary TRM can only be identified for a component if the direction linearly decays to the origin and the specimen is free from alteration during the experiment. As these criteria cannot be assessed for previously published paleointensity results, and as any high-field values for our new data are not clearly primary in origin, we have attempted to understand what might give rise to apparent high paleointensities. Given that lunar samples returned in Apollo capsules were exposed to a small, but potentially damaging magnetic field (Strangway et al., 1973), and given that perhaps the most reliable interpretation of our own Thellier–Thellier experiments is the low paleofield value recorded by 72215.262 we conducted an experiment to investigate the effect of a primary TRM (a possible lunar paleofield) with a secondary IRM overprint (spacecraft contamination). The results from this experiment (Section 4.2) indicate that such a magnetization scenario

can give rise to paleointensity results that qualitatively resemble those obtained for lunar samples, with Arai plots exhibiting a break in slope. The field in which the sample acquired a TRM was unrecoverable during the experiment, suggesting that it is possible that neither component (slope A or B) accurately represents the strength of a magnetic field in existence when lunar materials cooled through the Curie temperature. It has yet to be explored whether the adverse effects of an IRM overprint can be removed through AF demagnetization to yield a successful Thellier–Thellier experiment.

It is readily apparent from the data presented in this study that multi-component NRM behavior must be assessed and documented in order to accurately interpret the magnetizations of lunar samples. Therefore, sIRM methods that fail to identify and correctly characterize multiple components of an NRM are inadequate to measure remanent magnetic fields in lunar samples, and should not be used to infer a high-field era in early lunar evolution. Gattacceca and Rochette (2004), note that even after the removal of secondary (overprint) components via alternating field demagnetization the sIRM method cannot accurately determine the paleomagnetic field because it does not account for instances where residual fractions of NRM and IRM differ after the highest demagnetization step, and at the demagnetization step used to establish a relative paleointensity (typically, 20 mT).

The estimated absolute paleointensity for any sIRM measurement is subject to a poorly constrained scaling factor (f), which is dependent on parameters such as field strength, magnetic mineralogy, grain size, and grain shape. Earlier (Fuller and Cisowski, 1987) and recent work (Gattacceca and Rochette, 2004; Kletetschka et al., 2004, 2006; Yu, 2006) reach differing conclusions on the importance of these parameters; theory indicates that all should play a role. Relative paleointensities have been measured for different types of lunar rocks that have different mineralogy, grain shape, and size, and may have formed during different magnetic fields. If f depends on magnetic carrier (type, grain size, anisotropy) and/or field strength then the use of a constant scaling factor is inappropriate, and importantly, might affect the resulting temporal structure of the relative paleointensity data set. Furthermore, as a result of our re-evaluation of published absolute paleointensity data, the uncertainty in even an average single empirical lunar scaling factor (e.g. Cisowski et al., 1983; Kletetschka et al., 2004) is large because only 4 of the 14 samples used to calculate the scaling factor are considered acceptable. From this discussion we deem it inappropriate to provide estimates of absolute paleointensity for our sIRM measurements because of the ill-constrained lunar scaling factor, and the questionable association of the new sIRM measurements with primary TRMs. Authors who have recently applied the sIRM method (e.g., Garrick-Bethel and Weiss, 2007; Gattacceca and Rochette, 2004; Yu, 2006) acknowledge its shortcomings of limited precision for estimating the paleofield, in some cases providing no better than an order of magnitude estimate.

6.2.2. Impacts and shock

Clearly impacts, and therefore shock, have played a significant role in the formation of the lunar surface. All samples that have paleointensity measurements passing the reliability criteria set forth in this study have been extensively modified by shock-related events. For example, sample 15498 is a shock-lithified sample that was most likely heated in a high-field ejecta blanket (Christie et al., 1973; Gose et al., 1972). Cisowski et al. (1976, 1973, 1975) conducted a suite of experiments in the presence of a magnetic field (Earth's field) that demonstrate the possible adverse effects of low to moderate shock on the magnetic remanence for lunar materials. Cisowski et al. (1975) argue that SRM (shock remanent magnetization) is the likely source of NRM in certain regolith breccias and that shock may modify the primary remanence of many other samples.

Of particular interest is sample 62235, which has yielded a component of magnetization with an apparently high paleointensity in previous studies and our new results. A recent reexamination of previous work on 62235 by Fuller and Halekas (2008) suggests that the data are consistent with a small high-temperature TRM, accompanied by a strong SRM acquired in a later event. Our new data support this interpretation and clearly indicate that further examination of the role of shock on lunar samples is needed. In particular, Fuller and Halekas (2008) note that shock may be affecting the magnetic signature of lunar samples, even for samples where there are no strong petrological effects evident.

Analyses of lunar crustal magnetic fields indicate that impact processes govern the distribution of surface fields (e.g. Halekas et al., 2001; Hood et al., 2003; Lin et al., 1988; Richmond et al., 2005). Lunar Prospector Electromagnetic Reflectometer (e.g. Mitchell et al., 2008) and Magnetometer (e.g. Richmond and Hood, 2008) studies show that (1) the majority of the moon's surface has weak (<3 nT) surface fields, (2) impact basins have weaker magnetic anomalies than surrounding crust (Halekas et al., 2002, 2003), and (3) the strongest magnetic anomalies are antipodal to four large impact basins (Imbrium, Orientale, Crisium and Serenitatis) (e.g. Lin et al., 1988). The strong magnetic crustal fields antipodal to large impact basins have motivated the hypothesis that crustal magnetization is a result of hypervelocity impacts causing plasma clouds to compress and amplify pre-existing ambient magnetic fields (whether internal dynamo or inter-planetary magnetic field in origin) near the antipode of an impact site (e.g. Crawford and Schultz, 1991; e.g. Crawford and Schultz, 1999; Hood and Artemieva, 2007; Hood and Huang, 1991; Snkra et al., 1979). SRM may be acquired by pre-existing basement materials and/or ejecta at the antipode due to magnetization of due to increased pressure (2–10 GPa) from focused (1) seismic energy or (2) secondary impacts at the antipode from primary impact ejecta. Several studies (Hood and Artemieva, 2007; Hood and Huang, 1991) argue that the field amplification effects at the antipode are sufficiently large that the properties of the pre-existing ambient magnetic field are negligibly important, eliminating the need for a strong pre-existing field to produce magnetic anomalies at impact antipodes. In fact, the lack of even weak magnetic anomalies within the Imbrium basin (Halekas et al., 2002, 2003) supports the hypothesis that a strong ambient field did not exist during its formation (3.75–3.87 Ga (Stoffler and Ryder, 2001)).

6.3. An uneasy case for an early dynamo

Our new paleointensity data and our re-evaluation of published results indicate that inferred high paleointensities do not reflect magnetization of samples in a 3.9–3.6 Ga lunar dynamo-driven field. This inference is consistent with the general absence of strong magnetic anomalies associated with both the edges of Imbrium-aged basins and the mare basalts that formed in the 3.9–3.6 Gyr time period. In addition, the strong surface fields present problems for dynamo models, as originally pointed out by Hood et al. (1979). The 100 μT surface fields previously proposed for the 3.9–3.6 Ga interval, require core surface fields that are at least 100 times this value (assuming a dipolar surface field geometry), and a core Elsasser number that is difficult to reconcile with current understanding of dynamo-generated fields. Finally, an early dynamo driven by heat flow through the core-mantle boundary (Stegman et al., 2003) places severe constraints on the early thermo-chemical evolution of the Moon, that are relaxed in the absence of a high-field era.

SRM, not TRM, provides the most straightforward explanation for both observed lunar crustal anomalies and the paleointensity data. Unfortunately, both previous and modern paleomagnetic methods cannot differentiate between SRM and TRM, complicating lunar paleomagnetic interpretations, and clearly further work is needed to understand the role shock has played in the magnetization of lunar samples.

The existence of a lunar dynamo prior to 3.9 Ga is an open question. It is possible that the high temperature, low intensity component observed in some lunar samples may reflect magnetization in an earlier, weak (few micro-Tesla) field (Fuller and Halekas, 2008); however this has not yet been unequivocally demonstrated. Additionally the inferred paleointensities are low enough that magnetization in the ambient interplanetary magnetic field is plausible, negating the need for an intrinsic lunar field. Some support for a Nectarian or pre-Nectarian weak lunar surface field is provided by the distribution of crustal magnetic fields, particular those inside major basins (Mitchell et al., 2008), however the distribution and interpretation of these crustal fields is complex.

7. Conclusions

In summary, lunar paleointensity measurements to date do not support the previously proposed interpretation: that of a 3.9–3.6 Ga lunar dynamo. Compilation and analyses of lunar paleointensities are hindered by (1) the limited number of measurable samples, (2) the variety and quality of previous paleointensity experiments, and (3) the ambiguous interpretation of complex paleointensity results. There is not a single lunar paleointensity result (in this study or in the published literature) that passes the criteria of a successful and robust paleointensity experiment (relative or absolute) as applied to terrestrial samples (Gattacceca and Rochette, 2004; Selkin and Tauxe, 2000). Of the four samples measured here, one (76535) experiment failed due to alteration, another (60015) did not record a measurable paleointensity, the paleointensity of a third sample (72215) is most likely due to shock or IRM contamination during sample return rather than thermal remanent magnetization, and the complicated results of the fourth (62235) cannot be unambiguously interpreted as a thermal remanent magnetization. More importantly, there is no conclusive evidence that any measured paleointensities are original thermal remanent magnetizations for lunar samples, regardless of the measurement method used. Hence, all future lunar paleointensity studies need to demonstrate primary remanent magnetization through directional data prior to interpreting paleointensity as recording magnetization acquired in a lunar dynamo field. The absence of reliable absolute paleointensity measurements is particularly problematic as it renders relative paleointensity measurements unreliable, since they are scaled using absolute measurements. A re-evaluation of previous results and the new data presented here do not negate the existence of an early lunar dynamo; they merely demonstrate a lack of evidence for one. While a dynamo may have existed early in the Moon's history, the absence of dynamo-driven strong ($\sim$100 μT) surface fields during the 3.9–3.6 Ga period is more compatible with other surface and satellite magnetic field observations, presents fewer difficulties for lunar thermal evolution models and is easier to reconcile with current understanding of dynamo processes.

Acknowledgements

We thank the reviewers, Mike Fuller and anonymous, for insightful feedback and constructive suggestions. We would like to thank Rob Van der Voo, Mark Jellinek, and Jesse Lawrence for discussions, which improved the manuscript. We also thank Bruce Deck for aid in experimental set-up and execution. The work was supported under NASA Planetary Geology and Geophysics Grant NNG05GK34G.

Appendix A. Supplementary data

Supplementary data associated with this article can be found, in the online version, at doi:10.1016/j.pepi.2008.05.007.

References

Banerjee, S.K., Mellema, J.P., 1974. A new method for the determination of paleointensity from the A.R.M. properties of rocks. Earth and Planetary Science Letters 23 (2), 177–184.
Banerjee, S.K., Mellema, J.P., 1976. A solar origin for the large lunar magnetic field 4.0×10^9 yr ago? In: Proceedings of the 7th Lunar Science Conference, pp. 3259–3270.
Banerjee, S.K., Swits, G., 1975. Natural remanent magnetization studies of a layered breccia boulder from the lunar highland region. The Moon 14 (3–4), 473–481.
Brecher, A., Menke, W., Morash, K., 1974. Comparative magnetic studies of some Apollo 17 rocks and soils and their implications. In: Proceedings of the Fifth Lunar Science Conference, vol. 3, pp. 2795–2814.
Brecher, A., Vaughan, D., Burns, R., Morash, K., 1973. Magnetic and Mossbauer studies of Apollo 16 rock chips 60315,51 and 62295,27. In: Proceedings of the Fourth Lunar Science Conference, vol. 3, pp. 2991–3001.
Butler, R.F., 1992. Paleomagnetism: Magnetic Domains to Geologic Terranes. Blackwell Scientific, Boston, 336 pp.
Chowdhary, S.K., Collinson, D.W., Stephenson, A., Runcorn, S.K., 1987. Further investigations into lunar paleointensity determinations. Physics of the Earth and Planetary Interiors 49 (1–2), 133–144.
Christie, J.M., et al., 1973. Electron petrography of Apollo 14 and 15 breccias and shock-produced analogs. In: Proceedings of the Lunar and Planetary Science Conference, vol. 4, no. 365.
Cisowski, S.M., Collinson, D.W., Runcorn, S.K., Stephenson, A.A., 1983. A review of lunar paleointensity data and implications for the origin of lunar magnetism. Journal of Geophysical Research 88, A691–A704.
Cisowski, S.M., Collinson, D.W., Stephenson, A., Runcorn, S.K., 1982. A new look at lunar paleomagnetic data: Evidence for a well-defined lunar "magnetic Epoch" 3.65–3.85 GY B.P. Lunar and Planetary Science XIII, 107–108 (Abstract).
Cisowski, S.M., et al., 1976. Magnetic effects of shock and their implications for lunar magnetism (II). In: Proceedings of the 7th Lunar and Planetary Science Conference, pp. 3299–3320.
Cisowski, S.M., Fuller, M., Rose, M.F., Wasilewski, P., 1973. Magnetic effects of experimental shocking of lunar soil. In: Proceedings of the 4th Lunar and Planetary Science Conference, p. 3003.
Cisowski, S.M., Fuller, M., Wu, Y., Rose, M.F., Wasilewski, P., 1975. Magnetic effects of shock and their implications for magnetism of lunar samples. In: Proceedings of the 6th Lunar and Planetary Science Conference, pp. 3123–3141.
Cisowski, S.M., Hale, C., Fuller, M., 1977. On the intensity of ancient lunar fields. In: Proceedings of the 8th Lunar Science Conference, pp. 725–750.
Coe, R.S., Grommé, S.C., Mankinen, E.A., 1978. Geomagnetic paleointensities from radiocarbon dated lava flows on Hawaii and the question of the Pacific nondipole low. Journal of Geophysical Research 83, 1740–1756.
Collinson, D.W., 1985. Primary and secondary magnetizations in lunar rocks—implications for the ancient magnetic field of the Moon. Earth Moon and Planets 33 (1), 31–58.
Collinson, D.W., 1993. Magnetism of the Moon—a lunar core dynamo or impact magnetization. Surveys in Geophysics 14 (1), 89–118.
Collinson, D.W., Stephenson, A., Runcorn, S.K., 1973. Magnetic properties of Apollo 15 and 16 rocks. In: Proceedings of the Fourth Lunar Science Conference, vol. 3, pp. 2963–2976.
Crawford, D.A., Hollister, L.S., 1974. KREEP Basalt: a possible partial melt from the lunar interior. In: Proceedings of the Fifth Lunar Science Conference (Suppl. 5, Geochimica et Cosmochimica Acta), vol. 1, pp. 399–419.
Crawford, D.A., Schultz, P.H., 1991. Laboratory investigations of impact-generated plasma. Journal of Geophysical Research 96, 18807–18817.
Crawford, D.A., Schultz, P.H., 1993. The production and evolution of impact-generated magnetic fields. International Journal of Impact Engineering 14 (1–4), 205–216.
Crawford, D.A., Schultz, P.H., 1999. Electromagnetic properties of impact-generated plasma, vapor and debris. International Journal of Impact Engineering 23, 169–180.
Dunlop, D.J., Ozdemir, O., 1997. Rock Magnetism: Fundamentals and Frontiers. Cambridge Studies in Magnetism. Cambridge University Press, 573 pp.
Dymek, R.F., Albee, A.L., Chodos, A.A., 1975. Comparative petrology of lunar cumulate rocks of possible primary origin: Dunite 72415, troctolite 76535, norite 78235, and anorthosite 62237. In: Proceedings of the 6th Lunar and Planetary Science Conference, vol. 1, pp. 301–341.
Fuller, M., 1974. Lunar magnetism. Reviews of Geophysics and Space Physics 12 (1), 23–70.

Fuller, M., 1998. Lunar magnetism; a retrospective view of the Apollo sample magnetic studies. Physics and Chemistry of the Earth 23 (7–8), 725–735.
Fuller, M., Cisowski, S.M., 1987. Lunar paleomagnetism. In: Jacobs, J.A. (Ed.), Geomagnetism. Academic Press, San Diego, CA, pp. 307–456.
Fuller, M., Halekas, J., 2008. The role of impact related shock in lunar magnetism. Lunar and Planetary Science XXXIX (Abstract #1430).
Fuller, M., Meshkov, E., Cisowski, S.M., Hale, C., 1979. On the natural remanent magnetism of certain mare basalts. In: Proceedings of the 10th Lunar Science Conference, pp. 2211–2233.
Garrick-Bethel, I., Weiss, B.P., 2007. Early lunar magnetism. Lunar and Planetary Science XXXVI (Abstract #2405).
Gattacceca, J., Rochette, P., 2004. Toward a robust normalized magnetic paleointensity method applied to meteorites. Earth and Planetary Science Letters 227 (3–4), 377–393.
Gooley, R., Brett, R., Warner, J., Smyth, J.R., 1974. A lunar rock of deep crustal origin: Sample 76535. Geochimica et Cosmochimica Acta 38, 1329–1339.
Gose, W.A., Pearce, G.W., Strangway, D.W., Larson, E.E., 1972. On the applicability of lunar breccias for paleomagnetic interpretations. Earth, Moon, and Planets 5, 106.
Gose, W.A., Strangway, D.W., Pearce, G.W., 1973. A determination of the intensity of the ancient lunar magnetic field. The Moon 7, 196–201.
Hale, C.J., Fuller, M., Bailey, R.C., 1978. On the application of microwave heating to lunar paleointensity determination. In: Proceedings of the 9th Lunar and Planetary Science Conference, pp. 3165–3179.
Halekas, J., Lin, R.P., Mitchell, D.L., 2003. Magnetic fields of lunar multi-ring impact basins. Meteoritics and Planetary Science 38, 565–578.
Halekas, J.S., et al., 2001. Mapping of crustal magnetic anomalies on the lunar near side by the Lunar Prospector Electron reflectometer. Journal of Geophysical Research-Planets 106 (E11), 27841–27852.
Halekas, J.S., et al., 2002. Demagnetization signatures of lunar impact craters. Geophysical Research Letters 29 (13).
Helsley, C.E., 1970. Magnetic properties of lunar 10022, 10069, 10084 and 10085 samples. In: Proceedings of the Apollo 11 Lunar Science Conference, vol. 3, pp. 2213–2219.
Helsley, C.E., 1971. Evidence for an ancient lunar magnetic field. In: Proceedings of the Second Lunar Science Conference, vol. 3, pp. 2485–2490.
Hoffman, K.A., Baker, J.R., Banerjee, S.K., 1979. Combining paleointensity methods; a dual-valued determination on lunar sample 10017,135. Physics of the Earth and Planetary Interiors 20 (2–4), 317–323.
Hood, L.L., Artemieva, N.A., 2007. Antipodal effects of lunar basin-forming impacts: Initial 3D simulations and comparisons with observations. Icarus 193 (2), 485–502.
Hood, L.L., Coleman, P.J., Russell, C.T., Wilhelms, D.E., 1979. Lunar magnetic anomalies detected by the Apollo subsatellite magnetometers. Physics of the Earth and Planetary Interiors 20 (391–411), 53–57.
Hood, L.L., Huang, Z., 1991. Formation of magnetic anomalies antipodal to lunar impact basins: Two-dimensional model calculations. Journal of Geophysical Research 96 (B6), 9837–9846.
Hood, L.L., Mitchell, D.L., Lin, R.P., Acuna, H., Binder, A.B., 1999. Initial measurements of the lunar induced magnetic dipole moment using Lunar Prospector magnetometer data. Geophysical Research Letters 26, doi:10.1029/1999GL900487.
Hood, L.L., Richmond, N.C., Pierazzo, E., Rochette, P., 2003. Distribution of crustal magnetic fields on Mars: Shock effects of basin-forming impacts. Geophysical Research Letters 30, doi:10.1029/2002GL016657.
Hood, L.L., Russell, C.T., Coleman, P.J., 1981. Contour maps of the lunar remanent magnetic fields. Journal of Geophysical Research 86, 1055–1069.
Hood, L.L., et al., 2001. Initial mapping and interpretation of lunar crustal magnetic anomalies using Lunar Prospector magnetometer data. Journal of Geophysical Research-Planets 106 (E11), 27825–27839.
Kletetschka, G., Acuna, H., Kohout, T., Wasilewski, P., Connerney, J.E.P., 2004. An empirical scaling law for acquisition of thermoremanent magnetization. Earth and Planetary Science Letters 226, 521–528.
Kletetschka, G., et al., 2006. TRM in low magnetic fields: a minimum field that can be recorded by large multi-domain grains. Physics of the Earth and Planetary Interiors 154, 290–298.
Kletetschka, G., Kohout, T., Wasilewski, P.J., 2003. Magnetic remanence in the Murchison meteorite. Meteoritics & Planetary Science 38 (3), 399–405.
Lin, R.P., Anderson, K.A., Hood, L.L., 1988. Lunar surface magnetic field concentrations antipodal to young impact basins. Icarus 74, 529–541.
Mitchell, D.L., et al., 2008. Global mapping of lunar crustal magnetic fields by Lunar Prospector. Icarus 194 (2), 401–409.
Nagata, T., Fisher, R.M., Schwerer, F.C., 1972. Lunar rock magnetism. Earth, Moon, and Planets 4, 160–186.
Nagata, T., Fisher, R.M., Schwerer, F.C., 1974. Some characteristic magnetic properties of lunar materials. The Moon 9, 63–77.
Nagata, T., Fisher, R.M., Schwerer, F.C., Fuller, M., Dunn, J.R., 1973. Magnetic properties and natural remanent magnetization of Apollo 15 and 16 lunar materials. In: Proceedings of the Fourth Lunar Science Conference, vol. 3, pp. 3019–3043.
Norman, M.D., Duncan, R.A., Huard, J.J., 2006. Identifying impact events within the lunar cataclysm from ^{40}Ar–^{39}Ar ages and compositions of Apollo 16 impact melt rocks. Geochemica et Cosmochimica Acta 70 (24), 6032–6049.
Nunes, P.D., 1975. Pb loss from Apollo 17 glassy samples and Apollo 16 revisited. In: Proceedings of the 6th Lunar and Planetary Science Conference, pp. 1491–1499.
Pearce, G.W., Gose, W.A., Strangway, D.W., 1973. Magnetic studies on Apollo 15 and 16 lunar samples. In: Proceedings of the Fourth Lunar Science Conference, vol. 3, pp. 3045–3076.
Pearce, G.W., Hoye, G.S., Strangway, D.W., Walker, B.M., Taylor, L.A., 1976. Some complexities in the determination of lunar paleointensities. In: Proceedings of the 7th Lunar Science Conference, pp. 3271–3297.
Pearce, G.W., Strangway, D.W., Gose, W.A., 1972. Remanent magnetization of the lunar surface. In: Proceedings of the Third Lunar Science Conference, vol. 3, pp. 2449–2464.
Premo, W.R., Tatsumoto, M., 1992. U–Th–Pb, Rb–Sr, and Sm–Nd isotopic systematics of lunar troctolite cumulate 76535: Implications on the age and origin of this early lunar, deep-seated cumulate. In: Proceedings of the 22nd Lunar and Planetary Science Conference, pp. 381–397.
Richmond, N.C., Hood, L.L., 2008. A preliminary global map of the vector lunar crustal magnetic field based on Lunar Prospector magnetometer data. Journal of Geophysical Research 113 (E02010), doi:10.1029/2007JE002933.
Richmond, N.C., et al., 2005. Correlations between magnetic anomalies and surface geology antipodal to lunar impact basins. Journal of Geophysical Research-Planets 110 (E5).
Riisager, P., Riisager, J., 2001. Detecting multidomain magnetic grains in the Thellier palaeointensity experiments. Physics of the Earth and Planetary Interiors 125 (1–4), 111–117.
Runcorn, S.K., 1994. The early magnetic-field and primeval satellite of the Moon: Clues to planetary formation. Philosophical Transactions of the Royal Society of London, Series A 349, 181–196.
Runcorn, S.K., 1996. The formation of the lunar core. Geochimica et Cosmochimica Acta 60, 1205–1208.
Runcorn, S.K., et al., 1971. Magnetic properties of Apollo 12 lunar samples. Proceedings of the Royal Society of London Series A-Mathematical and Physical Sciences 325, 157–174.
Russell, C.T., Coleman, P.J., Lichtenstein, B.R., Schubert, G., 1974. The permanent and induced magnetic dipole moment of the moon. In: Proceedings of the Fifth Lunar Science Conference, vol. 3, pp. 2747–2760.
Ryder, G., Norman, M.D., 1980. Catalog of Apollo 16 rocks. Curator's Office Publication #52, 3: JSC #16904.
Ryder, G., Stoeser, D.B., Marvin, U.B., Bower, J.F., Wood, J.A., 1975. Boulder 1, Station 2, Apollo 17: Petrology and petrogenesis. The Moon 14, 327–357.
Schaeffer, O.A., Husain, L., 1974. Chronology of lunar basin formation. In: Proceedings of the Fifth Lunar Science Conference, vol. 2, pp. 1541–1555.
Schaeffer, O.A., Warasila, R., Labotka, T.C., 1982. Ages of Serenitatis breccias. Lunar and Planetary Science XIII, 685–686 (Abstract).
Schubert, G., Turcotte, D.L., Olson, P., 2001. Mantle Convection in the Earth and Planets. Cambridge University Press, 956 pp.
Selkin, P.A., Tauxe, L., 2000. Long-term variations in paleointensity. Philosophical Transactions of the Royal Society of London, Series A 358, 1065–1088.
Snkra, L.J., et al., 1979. Magnetic field and shock effects and remanent magnetism in a hyper-velocity impact environment. Earth and Planetary Science Letters 42, 127–137.
Sonett, C.P., Colburn, D.S., Currie, R.G., Mihalov, J.D., 1967. The geomagnetic tail, topology, reconnection and interaction with the Moon. In: Carovillano, R.L., McClay, J.F., Radoski, H.F. (Eds.), Physics of the Magnetosphere. Reidel, Dordrecht, pp. 461–484.
Stegman, D.R., Jellinek, M.J., Zatman, S.A., Baumgardner, J.R., Richards, M.A., 2003. An early lunar core dynamo driven be thermochemical mantle convection. Nature 421, 143–145.
Steiger, R.H., Jäger, E., 1977. Subcommission on geochronology: Convention on the use of decay constants in geo- and cosmochronology. Earth and Planetary Science Letters 36, 359–362.
Stephenson, A., 1993. 3-Axis static alternating-field demagnetization of rocks and the identification of natural remanent magnetization, gyroremanent magnetization, and anisotropy. Journal of Geophysical Research 98 (B1), 373–381.
Stephenson, A., Collinson, D.W., 1974. Lunar magnetic field palaeointensities determined by an anhysteretic remanent magnetization method. Earth and Planetary Science Letters 23, 220–228.
Stephenson, A., Collinson, D.W., Runcorn, S.K., 1974. Lunar magnetic field palaeointensity determinations on Apollo 11, 16, and 17 rocks. In: Proceedings of the Fifth Lunar Science Conference, vol. 3, pp. 2859–2871.
Stephenson, A., Runcorn, S.K., Collinson, D.W., 1977. Paleointensity estimates from lunar samples 10017 and 10020. In: Proceedings of the 7th Lunar and Planetary Science Conference, pp. 679–687.
Stoffler, D., Ryder, G., 2001. Stratigraphy and isotope ages of lunar geological units: Chronological standard for the inner solar system. Space Science Reviews 96, 9–54.
Strangway, D.W., Gose, W.A., Pearce, G.W., Carnes, J.G., 1973. Magnetism and the history of the Moon. In: Graham Jr., C.D., Rhyne, J.J. (Eds.), Magnetism and Magnetic Minerals-1972. American Institute of Physics, New York, pp. 1178–1196.
Sugiura, N., Strangway, D.W., 1980. Comparison of magnetic paleointensity methods using a lunar sample. In: Proceedings of the 11th Lunar and Planetary Science Conference, pp. 1801–1813.
Sugiura, N., Strangway, D.W., 1983a. Magnetic paleointensity determination on lunar sample 62235. Proceedings of the Thirteenth Lunar and Planetary Science Conference, Part 2, Journal of Geophysical Research 88 (Supplement), A684–A690.
Sugiura, N., Strangway, D.W., 1983b. Magnetic properties of lunar samples 60315 and 60018: Strongly magnetized breccias. Lunar and Planetary Science XIV, 759–760 (Abstract).

Sugiura, N., Strangway, D.W., Pearce, G.W., 1978. Heating experiments and paleointensity determinations. In: Proceedings of the 9th Lunar and Planetary Science Conference, vol. 3, pp. 3151–3163.

Sugiura, N., Wu, Y.M., Strangway, D.W., Pearce, G.W., Taylor, L.A., 1979. A new magnetic paleointensity value for a "young lunar glass". In: Proceedings of the 10th Lunar and Planetary Science Conference, pp. 2189–2197.

Tauxe, L., 1998. Paleomagnetic Principles and Practice. Modern Approaches in Geophysics, vol. 17. Kluwer Academic Publishers, Dordrecht, 299 pp.

Tauxe, L.T., Staudigel, H., 2004. Strength of the geomagnetic field in the Cretaceous Normal Superchron: New data from submarine basaltic glass of the Troodos Ophiolite. Geochemistry Geophysics Geosystems 5 (Q02H06), doi:10.1029/2003GC000635.

Tauxe, L.T., Yamazaki, T., 2007. Paleointensities. In: Kono, M. (Ed.), Treatise on Geophysics, Geomagnetism Volume. Elsevier, pp. 509–563.

Taylor, L.A., 1979. Paleointensity determinations at elevated temperatures: Sample preparation technique. In: Proceedings of the 10th Lunar and Planetary Science Conference, pp. 2183–2187.

Thellier, E., 1938. Sur l'aimantation des terres cuites et ses applications géophysique. Ann. Inst. Phys. Globe Univ. Paris 16, 157–302.

Thellier, E., Thellier, O., 1959. Sur l'intensité du champ magnétique terrestre dans le passé historique et géologique. Annales de Geophysique 15, 285–378.

Wasilewski, P., 1974. Possible magnetic effects due to fine particle metal and intergrown phases in lunar samples. The Moon 11, 301–311.

Watson, D.E., Larson, E.E., Reynolds, R.L., 1974. Microscopic and thermomagnetic analysis of Apollo 17 breccia and basalt: Feasibility of obtaining meaningful paleointensities of the lunar magnetic field. In: Proceedings of the 5th Lunar and Planetary Science Conference, pp. 827–829.

Wieczorek, M.A., et al., 2006. The constitution and structure of the lunar interior, New Views of the Moon. Reviews in Mineralogy & Geochemistry. Mineralogical Soc America, Chantilly, p. 221.

Williams, J.G., Boggs, D.H., Yoder, C.F., Ratcliff, J.T., Dickey, J.O., 2001. Lunar rotational dissipation in solid body and molten core. Journal of Geophysical Research 106 (E11), 27933–27968.

Yu, Y.J., 2006. How accurately can NRM/SIRM determine the ancient planetary magnetic field intensity? Earth and Planetary Science Letters 250 (1–2), 27–37.

Yu, Y.J., Tauxe, L.T., Genevey, A., 2004. Toward an optimal geomagnetic field intensity determination technique. Geochemistry Geophysics Geosystems 5 (2), doi:10.1029/2003GC000630.